

# **Gen IV Nuclear Energy Systems**

Gas-Cooled Fast Reactor (GFR) Decay  
Heat Removal Concepts

Idaho National Laboratory  
Brookhaven National Laboratory

September 2005



The INL is a U.S. Department of Energy National Laboratory  
operated by Battelle Energy Alliance

# **Gas-Cooled Fast Reactor (GFR) Decay Heat Removal Concepts**

**Idaho National Laboratory  
Brookhaven National Laboratory**

**September 15, 2005**

**Idaho National Laboratory  
Idaho Falls, Idaho 83415**

**Prepared for the  
U.S. Department of Energy  
Under DOE Idaho Operations Office  
Contract DE-AC07-05ID14517**

## Contributors

### **Idaho National Laboratory**

K. D. Weaver

### **Brookhaven National Laboratory**

L-Y. Cheng

H. Ludewig

J. Jo

## Table of Contents

<b>1. Introduction .....</b>	<b>1</b>
<b>2. Passive Decay Heat Removal for a 2400 MW Pin Core by Natural Circulation. 3</b>	
2.1 <i>RELAP5/ATHENA Model</i> .....	3
2.1.1 Reactor Model for Steady-State Initialization .....	8
2.1.2 Emergency Heat Exchanger System .....	13
2.1.3 Radiative Heat Transfer .....	14
2.1.4 Transient Boundary Conditions and Cases .....	16
2.2 <i>ATHENA Transient Analysis</i> .....	17
2.2.1 Transient Cases .....	17
2.2.1.1 Case 1 .....	18
2.2.1.2 Case 2 .....	18
2.2.1.3 Case 3 .....	18
2.2.1.4 Case 4 .....	19
2.2.2 Analysis of Transient Results .....	19
2.2.2.1 Heat Removal Rate of the Emergency Cooling System .....	19
2.2.2.2 Reactor Pressure .....	20
2.2.2.3 Guard Containment Pressure .....	20
2.2.2.4 Guard Containment Gas Temperature .....	21
2.2.2.5 Hot Assembly Fuel Temperature .....	22
2.2.2.6 Maximum Fuel Temperature .....	22
2.2.2.7 Helium Flow in Natural Circulation .....	24
2.2.2.8 Gas Temperature at Core Outlet .....	24
2.2.2.9 Gas Temperature at Core Inlet .....	24
2.2.2.10 Water Flow Rate in the HEATRIC Heat Exchanger .....	25
2.2.2.11 Water Temperature at the Outlet of the HEATRIC Heat Exchanger .....	25
2.2.2.12 Impact of Radiative Heat Transfer .....	27
2.3 <i>Summary and Conclusions</i> .....	28
2.4 <i>References</i> .....	29
<b>3. Effects of the Reactor Cavity Cooling System .....</b>	<b>30</b>
3.1 <i>ATHENA/RELAP5 Model</i> .....	30
3.2 <i>ATHENA Transient Analysis</i> .....	32
3.2.1 Transient Cases .....	32
3.2.2 Analysis of Transient Results .....	33
3.2.2.1 Heat Removal Rate of the Emergency Cooling System .....	33
3.2.2.2 Reactor Pressure .....	33
3.2.2.3 Guard Containment Pressure .....	34
3.2.2.4 Guard Containment Gas Temperature .....	35
3.2.2.5 Peak Fuel Temperature .....	35
3.2.2.6 Helium Flow in Natural Circulation .....	36
3.2.2.7 Gas Temperature at Core Outlet .....	37
3.3 <i>Summary and Conclusions</i> .....	38
3.4 <i>References</i> .....	38
<b>4. Modeling of the Power Conversion Unit (PCU) .....</b>	<b>39</b>

4.1	<i>GT-MHR Power Conversion Unit</i> .....	39
4.2	<i>Helium Brayton Cycle</i> .....	40
4.3	<i>Turbomachinery</i> .....	41
4.3.1	Turbine .....	41
4.3.2	Low and High Pressure Compressors .....	41
4.4	<i>Heat Exchanger</i> .....	41
4.4.1	Recuperator .....	42
4.4.2	Precooler and Intercooler .....	42
4.5	<i>Future Work</i> .....	42
4.6	<i>References</i> .....	42
5.	<b>Conclusions and Recommendations</b> .....	44

## 1. Introduction

Current research and development on the Gas-Cooled Fast Reactor (GFR) has focused on the design of safety systems that will remove the decay heat during accident conditions, ion irradiations of candidate ceramic materials, joining studies of oxide dispersion strengthened alloys; and within the Advanced Fuel Cycle Initiative (AFCI) the fabrication of carbide fuels and ceramic fuel matrix materials, development of non-halide precursor low density and high density ceramic coatings, and neutron irradiation of candidate ceramic fuel matrix and metallic materials. The vast majority of this work has focused on the reference design for the GFR: a helium-cooled, direct power conversion system that will operate with an outlet temperature of 850°C at 7 MPa.

In addition to the work being performed in the United States, seven international partners under the Generation IV International Forum (GIF) have identified their interest in participating in research related to the development of the GFR. These are Euratom (European Commission), France, Japan, South Africa, South Korea, Switzerland, and the United Kingdom. Of these, Euratom (including the United Kingdom), France, and Japan have active research activities with respect to the GFR. The research includes two main projects: the GFR design and safety project, and the GFR fuels/in-core materials/fuel cycle project.

Previous work performed on safety system design has included the analysis of a 600MWt block-type (cercer) core, and indicate that 1) a fully passively safe GFR design is possible, but the economics demonstrate a prohibitively high cost due to the fuel and fuel cycle; 2) more economical systems appear to have a common requirement of a containment backpressure for use in the passive/natural convection mode; 3) the injection of a heavy gas (e.g., nitrogen, carbon dioxide, etc.) greatly enhances natural convection, and reduces the absolute backpressure needed; 4) active systems (e.g., blowers) would require very little power ( $\sim 100\text{kW} \times 3$ ), and may show greater reliability as compared to their passive counterparts; and 5) a combined active/passive system with a minimal backpressure of 5 bar requires even less power ( $\sim 16\text{kW} \times 3$ ) for the active side, i.e., a blower is run for the first 24 hours of an accident, and then shuts down to allow solely natural convective cooling to occur for the remainder of the accident period. In addition to the block core, a 600MWt, low-pressure drop pin core was also examined, where purely natural convective cooling was used to remove the decay heat. Figure 1-1 shows the relationship of EHX pressure drop (y-axis) to decay power (x-axis) based on the desired outlet temperatures and coolants. Again, as can be seen in the figure, the use of a heavy gas greatly enhances the ability to remove the decay heat during postulated accidents.

The remainder of this report is a compilation of work performed during this fiscal year (FY05) on passive (natural convective) decay heat removal systems for a 2400MWt GFR pin core. This report satisfies the two Level 2 milestones, "Selection of one or more advanced concepts for GFR decay heat removal that will maintain the reactor in a safe condition during an accident" for the Idaho National Laboratory (workpackage G-I0401K01), and "Select one or more advanced concepts for GFR decay heat removal which will maintain the reactor in a safe condition during postulated accidents" for Brookhaven National Laboratory (workpackage G-Y0401K01), due on September 15, 2005.

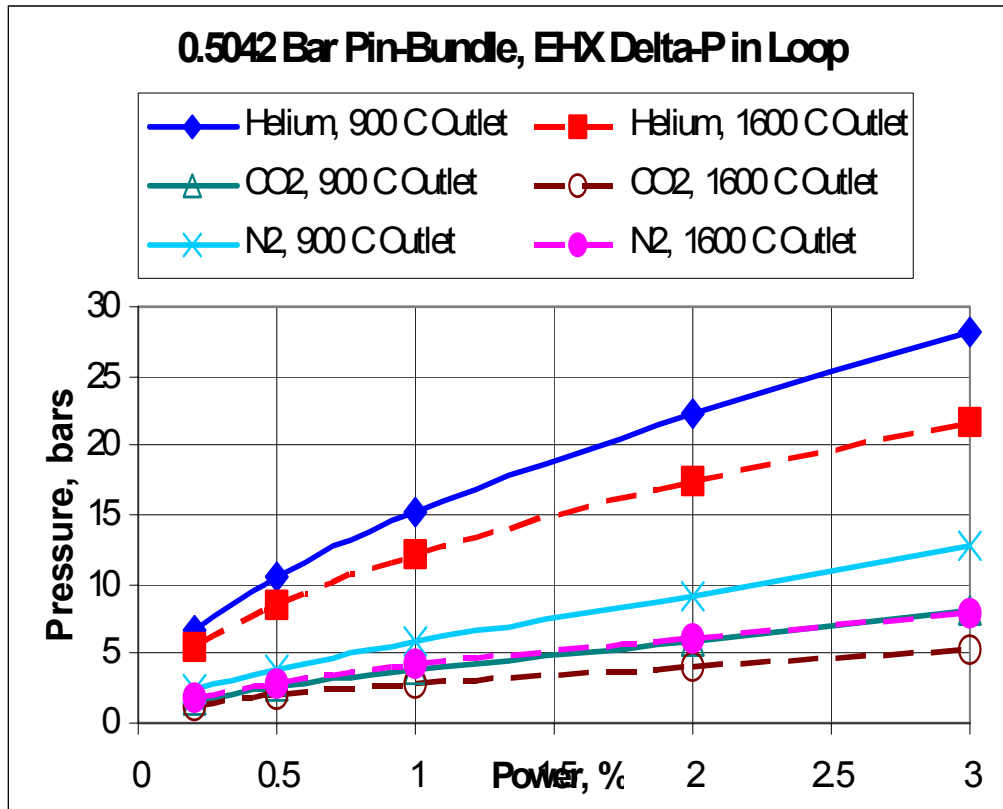


Figure 1-1 – Natural Convection for Pin-Bundle Core.

## **2. Passive Decay Heat Removal for a 2400 MW Pin Core by Natural Circulation**

A series of transient analysis using the system code RELAP5/ATHENA [2-1] has been performed to assess decay heat removal by natural circulation cooling under postulated accident conditions. The analysis is for a helium-cooled reactor of pin core design with a power density of 100 W/cc and a thermal power of 2400 MW. The objective is to ensure that the maximum fuel temperature remains within acceptable limits ( $< 1600^{\circ}\text{C}$ ) following a depressurization accident with scram and total loss of AC power.

The removal of decay heat from the core will follow the initiation of the depressurization accident in two steps. Initially, heat will be removed by a combination of flow coastdown due to inertia of the power conversion system and system depressurization caused by coolant flowing out of the break from the primary system. Following this step a self-sustaining method for long-term heat removal of the core will be required. A passive mode of heat removal relying on natural circulation cooling is investigated in this report. An emergency heat exchanger loop outside the reactor vessel will transfer energy from the reactor to an ultimate heat sink located outside the guard containment. By the opening of a check valve inline with the emergency heat exchanger a natural circulation flow path is established through the core and between the upper plenum and downcomer of the reactor vessel. Radiative heat transfer has also been included in the model to account for the exchange of thermal energy between heat structures by radiation.

In order for natural circulation cooling to function efficiently the primary system and the containment will need to be pressurized to ensure a sufficiently high coolant density. This will be accomplished by having a guard containment structure around the primary system. The main objective of the analysis reported here is to evaluate the effects of guard containment backpressure on the effectiveness of natural circulation cooling.

### **2.1 RELAP5/ATHENA Model**

A RELAP5 model of the reactor system has been constructed to address different parametric effects that influence the steady state and transient behavior of the pin core under natural circulation cooling at decay heat power levels. The model consists of two power conversion unit loops, an emergency heat exchanger loop with its heat sink, and a guard containment surrounding the primary system. The actual power plant will be constructed using four power conversion loops. However, in the RELAP model three loops are combined into one large loop (1800 MW), and one loop (600 MW) is isolated in order to correctly model the depressurization dynamics, since the leak flow will emanate from only one of the power conversion loops. This arrangement is shown schematically on Figure 2-1. Several volumes are used to represent the core and the pressure vessel, and the fuel and metal components are represented as heat structures. Thermal radiation is accounted for between the heat structures. The core has multiple axial and radial channels in order to represent both axial and radial power distributions. The shutdown and emergency cooling system is sized to handle 2% decay heat removal by natural circulation in a 4x50% configuration, i.e. four separate loops of 1% power capacity. In the RELAP5 model the emergency heat removal system is represented by one heat exchanger, which is sized to handle 2% of full power. Thus, once the decay heat reaches a level of 2 % of full power the emergency heat removal system should be able to handle the heat load. The heat



exchanger is based on the compact HEATRIC concept (i.e., a printed circuit heat exchanger). The primary side coolant is helium, which is used to cool the core, and the secondary side uses pressurized water as a working fluid. The ultimate heat sink consists of a large water tank located outside the guard containment building.

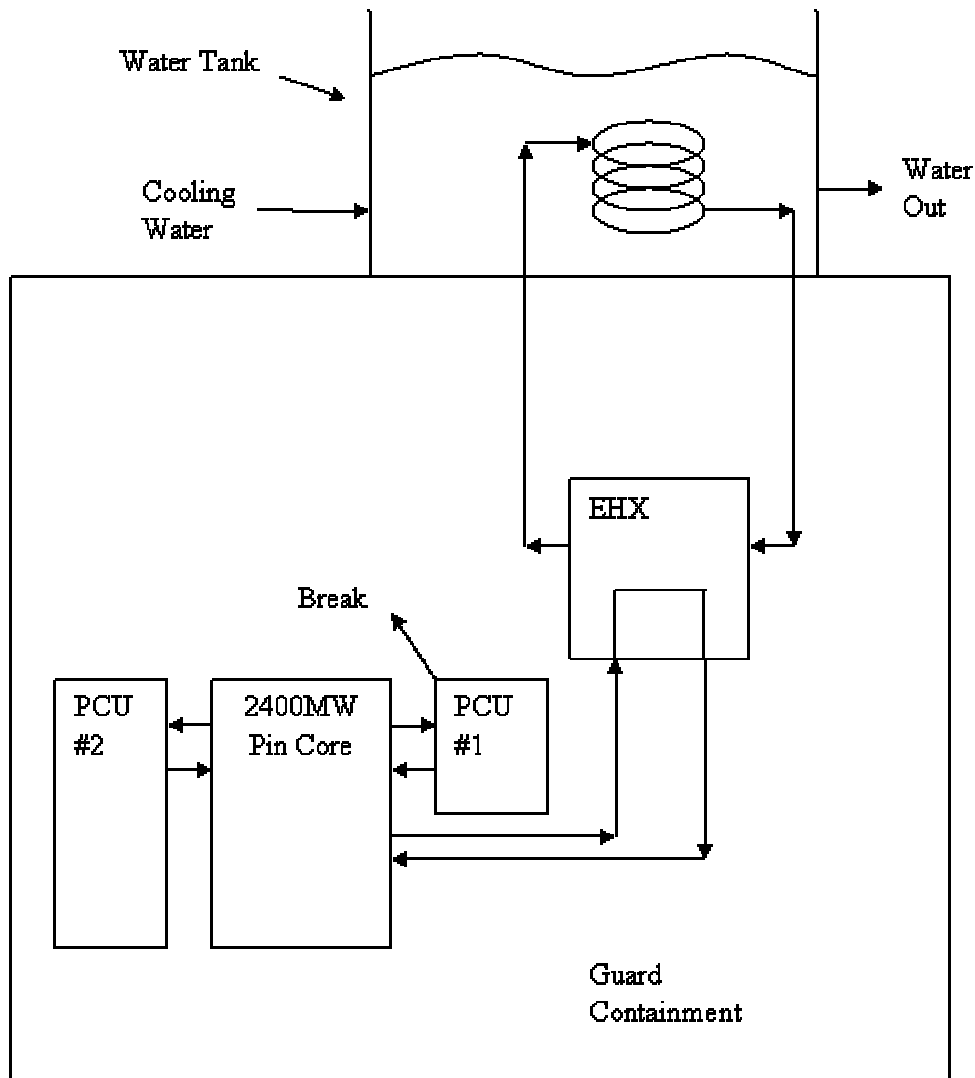


Figure 2-1 – Schematic Model of the Reactor System and the Associated Emergency Cooling Loop.

Details of the heat structures used in the RELAP model for convective and radiative heat transfer are shown in Figure 2-2. The core model consists of three radial zones and ten axial zones. The three radial zones include a hot assembly, a hot zone, and an average zone. Each of the radial zones is divided into ten axial zones. Power generation in each zone is obtained from output of the reactor physics analysis. Beyond the core there is a radial reflector, shield, core barrel, reactor pressure vessel wall and support structure, and finally the guard containment wall. It is

seen that explicit heat generation is only modeled in the core volumes. Heat generation in the other volumes is of marginal importance, and these structures act only as thermal capacitors.

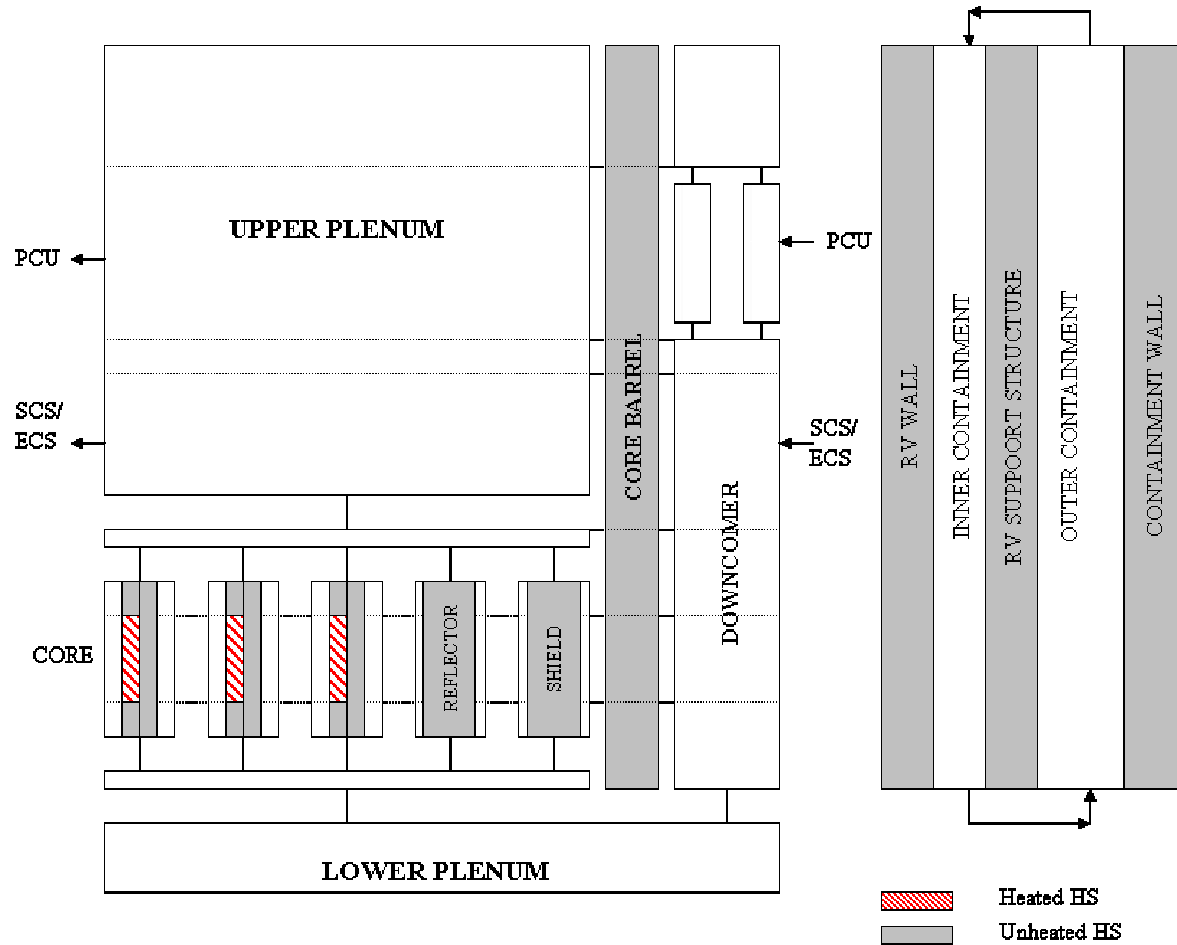


Figure 2-2 – Reactor Vessel and Guard Containment Heat Structures.

The model for determining the heat transfer due to radiation is shown in Figure 2-3. This model allows for radial radiation heat transfer only, and couples the hot inner core parts to the cooler outer parts. Figure 2-3 is thus a radial section through the core and associated guard containment wall, since these are the heat structures involved in the heat transfer process. It is seen that the fuel pins radiate to the assembly cans, which in turn radiate to each other. At the outer core boundary the element cans radiate to the inner reflector surface, which radiates to the radial shield. Finally the shield radiates to the core barrel, which radiates to the reactor pressure vessel, and it finally radiates to the guard containment wall. It is assumed that the guard containment wall is kept at a constant temperature by a thermal management system embedded in the wall.

It is clear from the above discussion that the core heat transfer model has both a convective and a radiative component. Convectively, heat is removed from the core by helium gas flowing up along the fuel pins. This mechanism is either forced or natural convection. The second heat transfer mechanism is radiation from the hotter parts of the core to the cooler parts of the core.

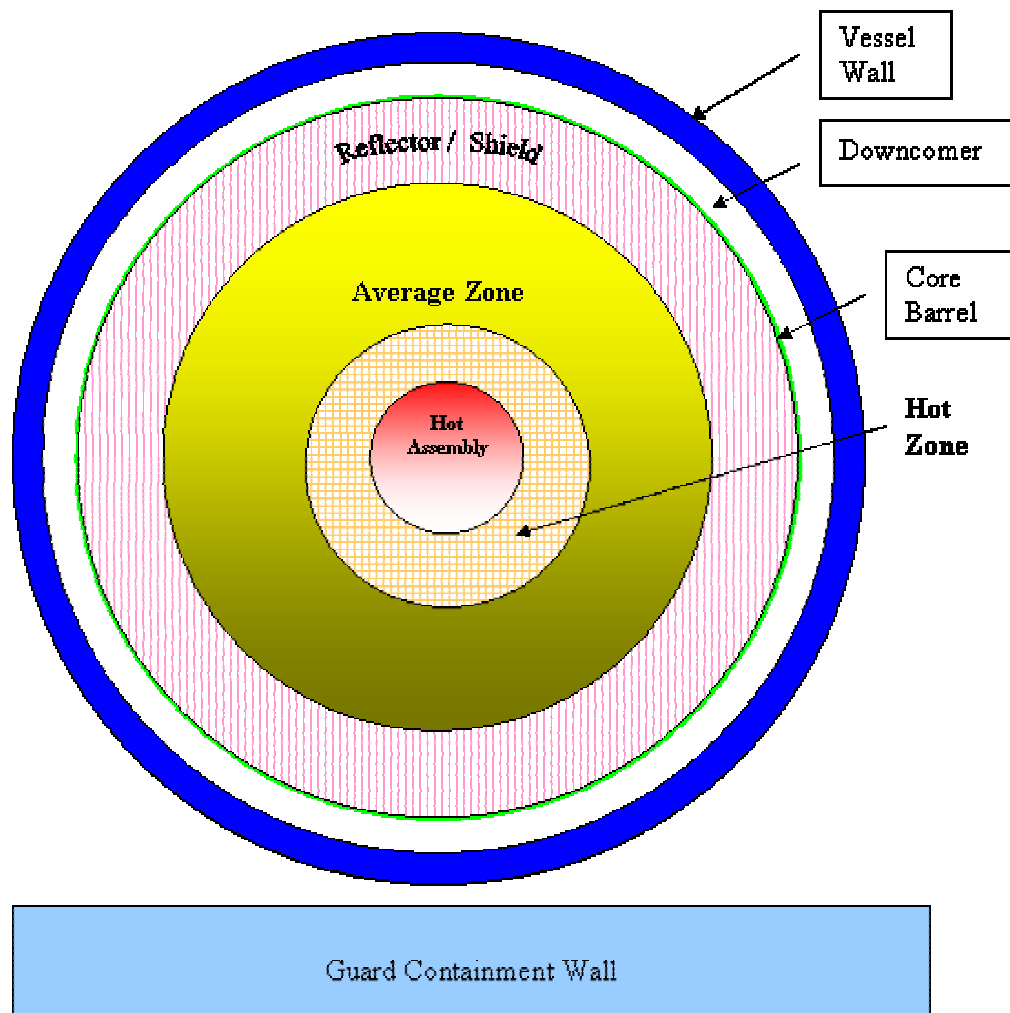


Figure 2-3 – Heat Structures for Radiation Heat Transfer.

Details of the primary system and the power conversion unit (PCU) are shown in Figure 2-4. It is seen that all the components of the power conversion unit are represented. However, at this stage the actual turbine, compressors, and generator models are not complete. The actual models for these components, including performance maps and inertia terms, will be added at a later date. The primary system depressurization is assumed to take place from a failure in the cold inlet duct of the primary circuit. This location is close to the point of highest primary system pressure (actually located at the exhaust of the high pressure compressor outlet). Also shown in Figure 2-4 is the guard containment structure into which the primary coolant exhausts at the time of the break.

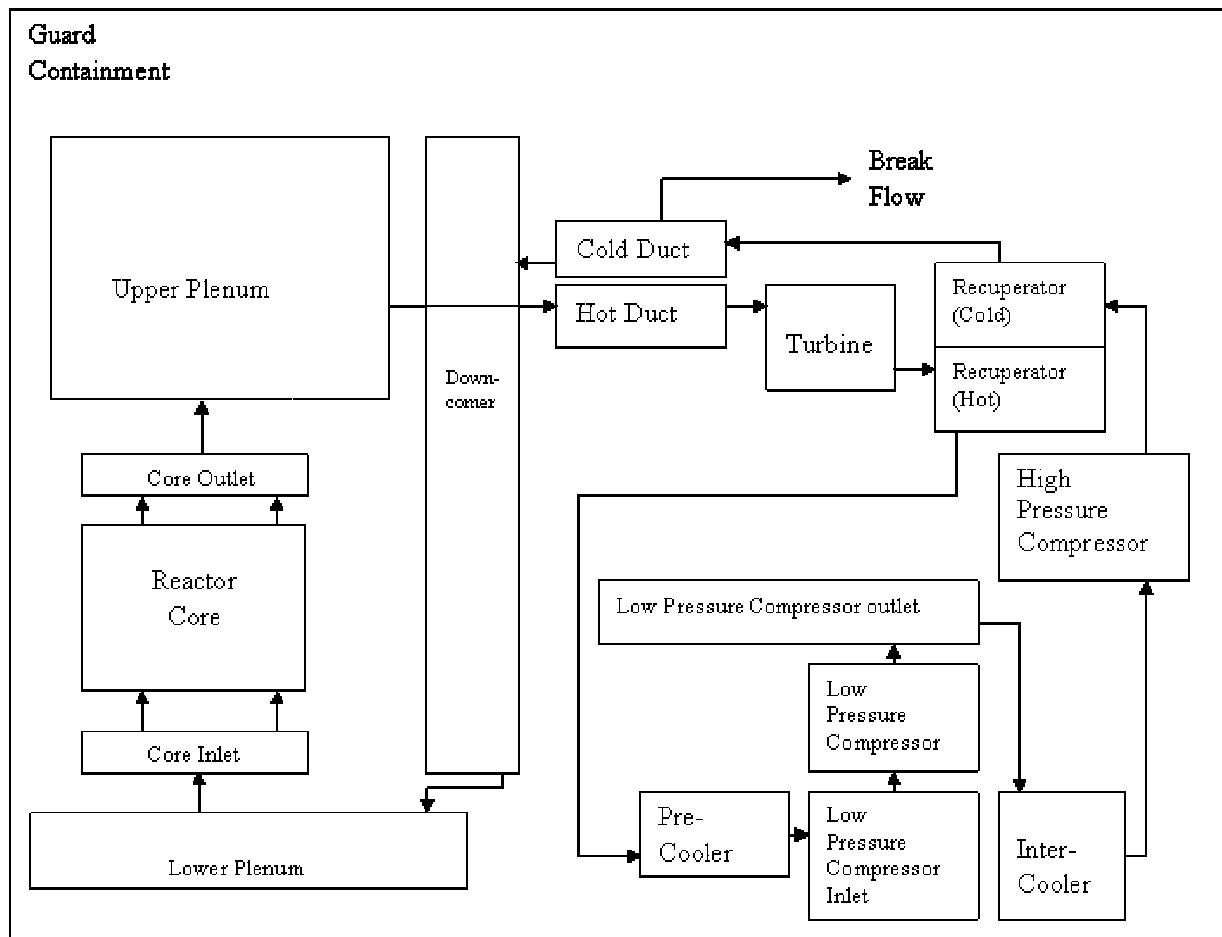


Figure 2-4 – Reactor Vessel and Power Conversion Unit Volume arrangement.

Details of the volume representation of the Shutdown Cooling System/Emergency Cooling System (SCS/ECS) are shown in Figure 2-5. The intermediate heat exchanger is based on the HEATRIC concept, and is shown in the horizontal orientation. A vertical orientation was also examined in the series of analysis reported below. The inlet and outlet of the SCS/ECS loop is connected to the upper plenum and the downcomer of the reactor pressure vessel respectively. Although the blower volume is explicitly modeled, the actual blower rotating components are not included at this stage. The inertia of the drive motor and/or the possible availability of backup battery power both of which could assist in forcing coolant to circulate around the primary circuit are thus not included in this analysis. This capability will be included in the next stage of the analysis.

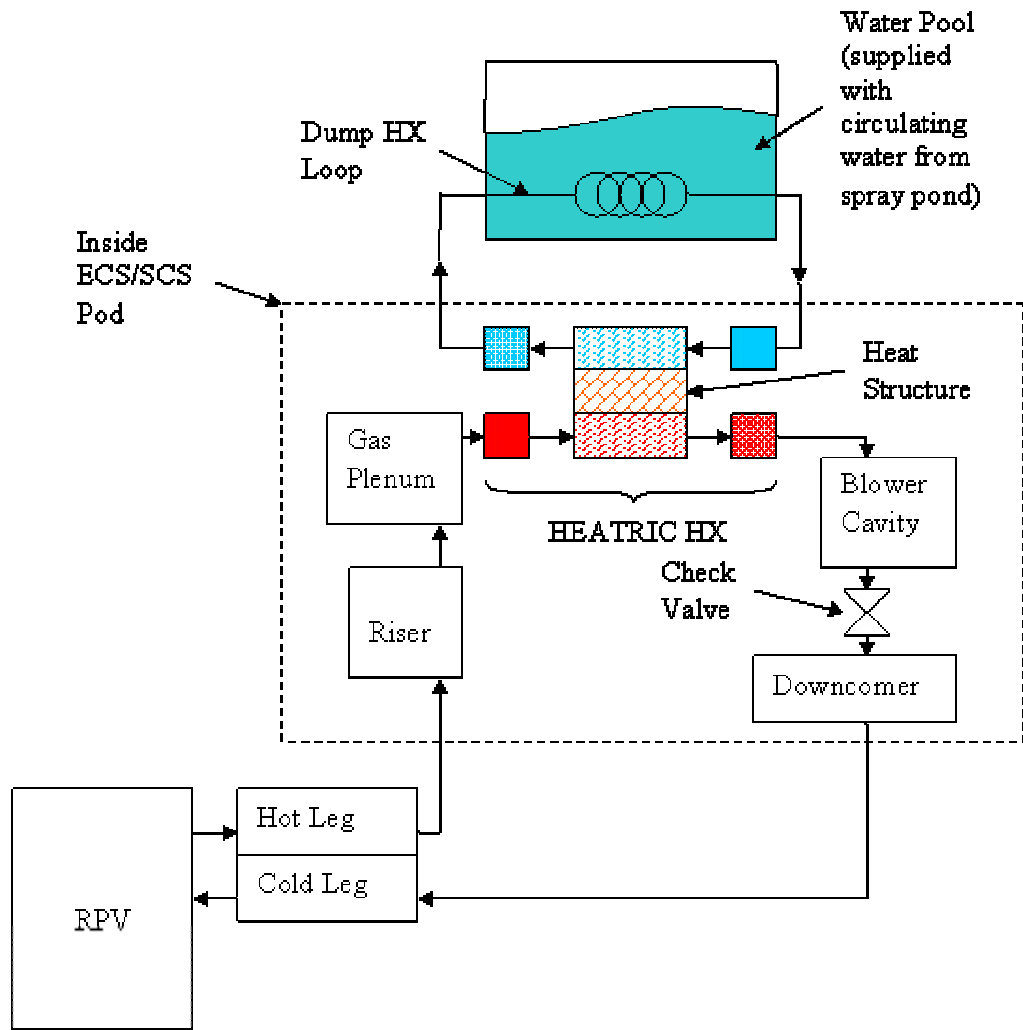


Figure 2-5 – Shutdown Cooling System/Emergency cooling System Volume arrangement.

### 2.1.1 Reactor Model for Steady-State Initialization

As shown in Figure 2-4, the RELAP model represents an integrated depiction of the primary and power conversion loops. Table 2-1 provides a summary of the geometric parameters of the inter-connecting volumes that represent different parts of the reactor vessel, and Table 2-2 provides the geometry and initial conditions for one unit of the 600MW PCU.

Table 2-1 – Reactor Vessel Geometry

Component	RELAP5 Volume #	Length (m)	Area (m <sup>2</sup> )	H <sub>D</sub> (m)
Upper Downcomer	047	3.241	6.775	0.61
Middle Downcomer	045 & 046 (in parallel)	4.5	3.3875	0.61
Lower Downcomer	050	7.627	6.775	0.61
Lower Plenum	051	2.68	33.65	6.71
Core Inlet	052	0.3	17.16	4.68
Average Zone	053	3.347*	6.2487	0.0122
Hot Zone	054	3.347*	0.9626	0.0122
Hot Assembly	055	3.347*	0.1050	0.0122
Core Outlet	056	0.5	17.16	4.68
Upper Plenum	058	11.5	35.36	6.71
Radial Reflector	032	3.347	0.0154	0.0122
Radial Shield	034	3.347	0.0103	0.0122

\* Includes lower and upper reflectors – 1.0m each.

Table 2-2 – PCU Geometry\* and Initial Conditions

Component	Length (m)	Volume (m <sup>3</sup> )	Area (m <sup>2</sup> )	Orientation (Deg)	Hydraulic Diameter (m)
Hot Duct	7.4	11.88484921	1.6060607	0	1.43
Turbine	4.2	2.04	0.4857143	90	0.786404
Turb - Recu	1.3848	0.6924	0.5	-90	0.797885
Recuperator	2.8152	59.5	21.135266	-90	0.009164
Recu - Prec	10.95	5.475	0.5	-90	0.797885
Precooler	4.73	142.4	30.105708	-90	0.009164
LPC duct	4.9	11.78588119	2.4052819	90	1.75
LPC inlet	2.38	14.23918074	5.982849	90	2.76
LPC	4.2	2	0.4761905	90	0.778656
LPC outlet	4.9	21.3	4.3469388	-90	2.352593
Intercooler	4.73	139.8	29.556025	-90	0.009164
Intc - HPC	9.63	4.815	0.5	90	0.797885
HPC	4.2	2	0.4761905	90	0.778656
HPC-Recu	2	1	0.5	0	0.797885
Recuperator	2.8152	59.5	21.135266	90	0.009164
Recu - Cduct	2.8152	1.4076	0.5	-90	0.797885
Cold Duct	7.4	13.94867138	1.8849556	0	0.6
Total Volume		493.7885825			

\* Geometry is for one 600MW unit.

Component	Volume Nodes	Temp (C)	Temp (K)	Pressure (MPa)
Hot Duct	1-4	848	1121.15	7.07
Turbine	5-7	678	951.15	4.84
Turb - Recu	8	508	781.15	2.61
Recuperator	9-10	319	592.15	2.59
Recu - Prec	11-13	130.3	403.45	2.58
Precooler	14-17	78.3	351.45	2.56
LPC duct	18-19	26.4	299.55	2.55
LPC inlet	20	26.4	299.55	2.55
LPC	21-23	66.9	340.05	3.43
LPC outlet	24-25	107.5	380.65	4.31
Intercooler	26-29	66.8	339.95	4.29
Intc - HPC	30-32	26	299.15	4.28
HPC	33-35	68.2	341.35	5.76
HPC-Recu	36	110.3	383.45	7.24
Recuperator	37-38	299	572.15	7.2
Recu - Cduct	39-40	488	761.15	7.16
Cold Duct	41-44	488	761.15	7.16

The following is a list of reactor parameters used in the model and is based on the ANL input database for the core design [2-2].

Reactor power = 2400 MWt  
System pressure = 7.0 MPa  
Core  $\Delta P = 5.2 \times 10^4$  Pa  
Helium flow = 1249 kg/s  
Inlet temperature = 480°C  
Outlet temperature = 850°C

The corresponding fuel subassembly parameters are listed in the following.

Number of hexagonal subassemblies = 418 (including 61 control assemblies)  
Number of fuel pins per subassembly = 271 (234 in control assemblies)  
Pin diameter = 9.65 mm [2-3]  
Clad (SiC) thickness = 1.0 mm [2-3]  
Radial gap (helium) = 0.1 mm [2-3]  
Fuel pellet (UC) diameter = 7.45 mm [2-3]  
Total coolant flow area = 9.1 m<sup>2</sup>  
Channel height = 3.34 m (fissile height = 1.34m)  
Hydraulic diameter = 12.2 mm  
Number of spacer grid assumed = 9  
Spacer grid loss coefficient = 0.65  
Flat-to-flat (outside) of hexagonal subassembly = 215 mm  
Hexagonal wall thickness = 3.7 mm

Thermal properties of UC and SiC used in the analysis are listed in Table 2-3. Preliminary physics calculation from ANL [2-3] indicated that reactor power is distributed between the core and the radial reflector/shield in a ratio of 99.65 % : 0.35 %. Since the energy deposition outside the core is negligible 100% of power is assumed to deposit in the three core zones. A flow split of 99.65% : 0.35% is assumed between the core and the radial reflector/shield. The reactor core is divided into a hot assembly, hot zone, and an average zone.



Table 2-3 – Properties of Fuel and Clad for the Pin Core

Fuel – UC

Density =  $13.61 \times 10^3 \text{ kg/m}^3$

Thermal Conductivity =  $21.6 \text{ W/m-K}$

Specific Heat =  $201 \text{ J/kg-K}$

Clad - SiC

Density =  $3210 \text{ kg/m}^3$

Thermal Conductivity:

Temperature (K)	Thermal Conductivity (W/m-K)
673	25.12
873	21.77
1073	18.42
1273	16.12
1473	13.40

Specific Heat:

Temperature (K)	Specific Heat (J/kg-K)
600	1050
900	1170
1200	1250
1500	1320

The pertinent parameters associated with these zones are given below:

	Hot Assembly	Hot Zone	Average Zone
Number of Assemblies:			
Regular Assembly	6	48	303
Control Assembly	0	7	54
Power Fraction (%)	1.7	14.1	84.2
Relative Radial Power Shape	1.31	1.21	0.967

The inclusion of the hot assembly as one of the three zones in the core is to simulate the effect of pin peaking within the hot zone. The assumed peaking is  $\sim 8\%$   $((1.31-1.21)/1.21)$ . Each region is sub-divided into 10 axial nodes with mid-core symmetry and a cosine axial power shape. The bottom and top nodes represent the axial reflectors (1 m in length) and no heat generation is assumed there. The axial power factors in the fueled region, from inlet to mid-core are: 0.82 (0.101m), 0.91 (0.168m), 1.04 (0.202m), 1.12 (0.202m), where the length of each node is in parenthesis. The fuel pins are modeled as cylindrical heat structures with three radial zones, fuel,

gas gap, and clad. In parallel with the core channels is the radial reflector/shield volume with its own hydraulic channel and heat structure. Details of these passive heat structures (no internal heat generation) are discussed later in relation to the modeling of radiation heat transfer.

### 2.1.2 Emergency Heat Exchanger System

Under natural circulation cooling decay power is removed by an in-vessel heat exchanger of HEATRIC design. A secondary loop using pressurized water transports the thermal energy, again by natural circulation, to an externally located ultimate heat sink. For this analysis the emergency heat exchanger system is modeled after an MIT design, shown in Figure 2-5. The HEATRIC heat exchanger consists of alternating layers of helium and pressurized water counter-current micro-channels. The HEATRIC heat exchanger is represented in the RELAP5 model as a plate heat structure separating the counter-current primary and secondary fluids. The secondary heat exchanger, located in the ultimate heat sink, consists of a tube and shell design with ten tube passes and one shell pass. The shell side is a water tank that represents an ultimate heat sink. The tank is assumed to be very large, and if necessary can be refilled. Below is a summary of the heat exchanger input data.

Working fluid = H<sub>2</sub>O pressurized to 9 MPa

Length of heat transfer surface = 0.3m

Plate thickness = 0.0037m

Heat transfer area = 2360m<sup>2</sup>

Flow area on the primary and secondary side = 6.01m<sup>2</sup>

Hydraulic diameter of flow channel = 0.003055m

Plate conductivity is based on Alloy 800H,

$$K_{\text{mat}}(T) = 6.8393 + 0.015577T,$$

where  $K_{\text{mat}}$  is the thermal conductivity in W/m-s and T is the temperature in K.

The arrangement of the SCS/ECS heat exchanger as it is located in a pod in the guard containment is shown in Figure 2-6.

The following additional; assumptions were made regarding the operation of the emergency cooling system:

- 1) The HEATRIC flow channels were orientated in the vertical direction. The original design had horizontal flow channels. However initial calculations showed a period of steam void formation at the start of heat transfer to the water side. For the calculations presented in this report the flow channels were oriented vertically to ease the establishment of natural circulation flow on the water side.
- 2) The difference in height between the core mid-plane and the mid-plane of the emergency heat exchanger is 16 m.
- 3) The height between the emergency heat exchanger mid-plane and the tube heat exchanger mid-plane located in the ultimate heat sink is 8.5 m.
- 4) The ultimate heat sink tank is supplied by an external water supply at a rate of 355.2 kg/s at a temperature of 30° C.

- 5) The external water tank, representing the shell side of the secondary heat exchanger, is open to atmosphere and is assumed to have a height of 10m and a flow area of  $78.54\text{m}^2$ .
- 6) The tube side of the secondary heat exchanger is made up of 100 tubes with ID =  $0.03505\text{m}$ , OD =  $0.04216$  and 10 tube passes. Total flow area =  $0.09649\text{m}^2$  and total heat transfer area =  $425.14\text{m}^2$  (total heat transfer length =  $10 \times 3.21\text{m}$ ).

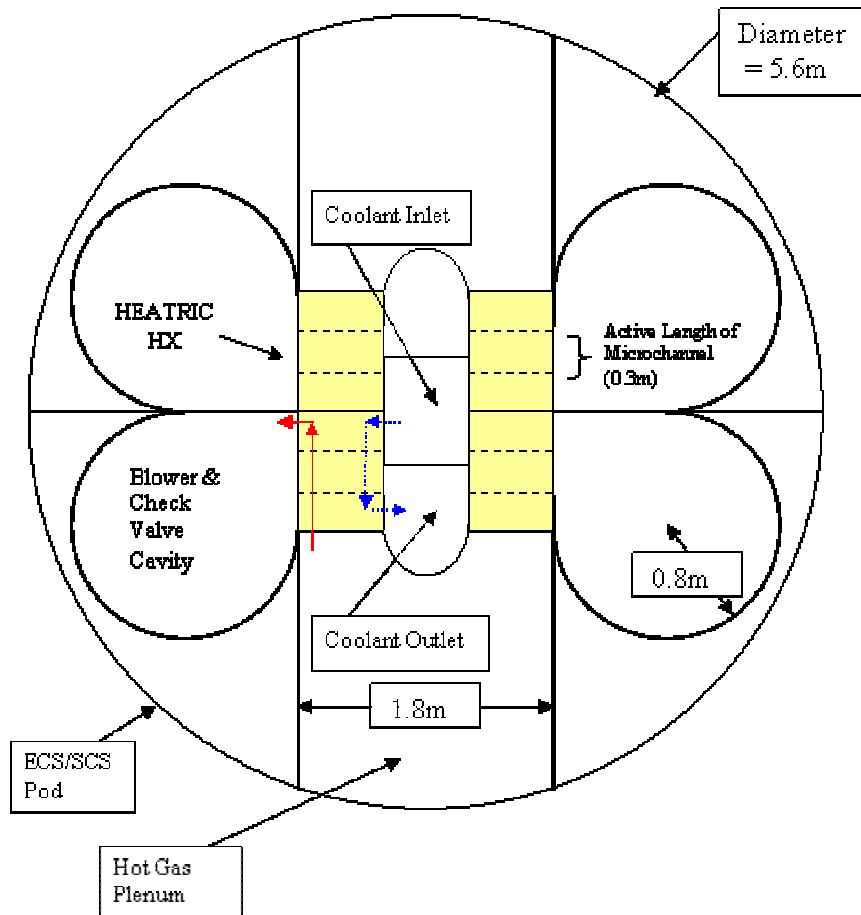


Figure 2-6 – SCS/ECS heat exchanger located in a pod within the guard containment.

### 2.1.3 Radiative Heat Transfer

The incorporation of radiation heat transfer among heat structures inside the reactor vessel provides an additional means of distributing thermal energy from hotter parts to cooler parts of the reactor. A simplified approach that is consistent with the lumped representations of fuel pins and assembly cans has been adopted to model the transfer of heat by radiation from fuel pins to the surrounding assembly cans and subsequently from one zone of the core to the next.

The heated heat structures (HS), i.e. the fuel pins, identified in Figure 2-2 is the source of energy and the unheated heat structures are other components that participate in the exchange of thermal energy by radiation. By assumption the zone of influence of radiation heat transfer is limited to the cylindrical section that coincides with the vertical extent of the fueled region of the core. As

an example, though the core barrel extends to the upper plenum, only the lower portion between the lower and upper boundaries of the fueled zone (1.347m in height) participates in radiation heat transfer.

The corresponding radiation heat transfer surfaces considered in the ATHENA model of the pin core are:

1. Fuel pins in each core zone (hot assembly, hot zone, and average zone, as shown in Figure 2-3) radiate to the corresponding hexagonal (hex) cans in the zone.
2. Hot assembly hex can radiates to hot zone hex can.
3. Hot zone hex can radiates to average zone hex can.
4. Average zone hex can radiates to radial reflector.
5. Radial reflector radiates to radial shield.
6. Radial shield radiates to core barrel.
7. Core barrel radiates to vessel wall.
8. Vessel wall radiates to vessel support structure.
9. Vessel support structure radiates to guard containment wall.

Once the radiating surfaces have been identified the other parameter of interest for radiation heat transfer is the view factor. In ATHENA the two rules that govern the definition of view factors for two interacting surfaces are:

$$A_i F_{ij} = A_j F_{ji}$$

$$\sum F_{ij} = 1 \text{ (For a given } i \text{ sum over } j)$$

where,

$A_i$  = area of radiating surface  $i$

$F_{ij}$  = view factor from surface  $i$  to surface  $j$

In this report the view factors for a given pair of radiating surfaces ( $A_i$  and  $A_j$ ) are evaluated by assuming that the two surfaces are two-dimensional concentric cylinders. According to the conceptualized radiating surfaces shown in Figure 2-3, the inner cylinder ( $A_1$ ) sees 100% of the outer cylinder ( $A_2$ ) and this gives  $F_{12} = 1$  that enables the determination of the rest of view factors for the pair of surfaces  $A_1$  and  $A_2$ . The situation for radiative transfer between the fuel pins and the surrounding hex can walls is a little different. In this case the fuel pins have a total surface area ( $A_1$ ) greater than the corresponding surface area of the hex cans ( $A_2$ ) and  $F_{21}$  is set to unity instead. Physically the interpretation of setting  $F_{21} = 1$  (hex can to fuel pin) is equivalent to treating the hex can as seeing 100% of the fuel pins while the fuel pins only see part of the hex can surface because the fuel pins see each other. This interpretation is consistent with the use of one lumped fuel pin to represent all the fuel pins in a core zone, i.e. fuel pins radiate to each other to achieve the same temperature at each axial location in a particular core zone.

Some of the input parameters for the heat structures that participate in radiation heat transfer are summarized below.

Radial reflector:

Inner radius = 2.4265m

Outer radius = 2.6955m

Material = Inconel

Radial shield:

Inner radius = 2.8175m

Outer radius = 3.2785m

Material = Inconel

Core barrel:

Inner radius = 3.355m

Outer radius = 3.38m

Material = stainless steel

Reactor vessel wall:

Inner radius = 3.6856m

Outer radius = 3.965

Reactor support structure:

Inner radius = 5.77m

Outer radius = 6.67m

Material = concrete

Guard containment wall:

Wall thickness = 0.02m

Material = concrete

An arbitrarily thin wall was used to simulate a wall that is close to the temperature of the outside temperature of 30 deg C. The boundary condition prescribed for the guard containment wall is an approximation to the design assumption that the guard containment wall is kept at a constant temperature by a thermal management system embedded in the wall.

The transient results indicate that the main effect of radiative heat transfer is the redistribution of energy among heat structures internal to the vessel. Radiative heat transfer to the guard containment wall is insignificant because of relatively low reactor vessel wall temperature.

#### **2.1.4 Transient Boundary Conditions and Cases**

In order to carry out a transient analysis of a thermal-hydraulic system both initial and boundary conditions need to be specified. In the cases to be considered here the following conditions will be specified:

- 1) Reactor initially at full power.
- 2) A 0.00645 m<sup>2</sup> (1.0 in<sup>2</sup>) rupture in the number one loop (600 MW) of the PCU cold leg initiates the transient.

- 3) Appropriate volumes represent power conversion unit, but no actual turbo-compressor model is included in the model.
- 4) Transient response of the turbo-compressor unit is modeled by linearly reducing the flow from the PCU into the primary loop. A ramp down time of 180 s. was assumed.
- 5) Guard containment volume is an input variable the magnitude of which is to be determined by the results of the transient analysis. Initially pressure and temperature were assumed to be 1 atmosphere and 30° C. The guard containment outside wall temperature was assumed to be at a steady state value of 30° C. It is assumed that the temperature is maintained by an outside independent heat removal system.

The primary objective of this analysis is to determine the volume and final temperature and pressure of the guard containment that result in acceptable core long term cooling of the core. Acceptable cooling of the core is defined by the conditions that result in the maximum hot pin surface temperature being below 1800 K. By varying the guard containment volume the final pressure in the guard containment also varies, and this value determines the density and thus the mass flow rate of the coolant flowing through the core. Higher guard containment pressures result in higher coolant mass flow rates and thus more efficient cooling. However, they also imply thicker guard containment walls and thus potentially more costly structures.

## **2.2 ATHENA Transient Analysis**

The first step of a transient analysis was to establish a steady-state at 100% power. The current models of the PCU do not include a compressor component and so initial flow is established by imposing upstream and downstream pressures in the reactor vessel, given the system pressure of 7.0MPa and a core pressure drop of  $5.72 \times 10^4$  Pa. With a helium inlet temperature of 480°C, the spacer loss coefficient is adjusted until an outlet temperature of 850°C is reached at the outlet of the reactor.

A transient case is run as a restart of the steady-state case from time zero. Simultaneously the restart case establishes new connections to the RPV at time zero. These include new flow junctions with the PCU via the cold and hot ducts and the guard containment via the break junction (simulated by a trip valve). Specifically the restart input file contains information for the break junction (flow area), the guard containment (volume, initial pressure and temperature), the PCU initial pressure and temperature distribution, time-dependent junction velocity between PCU and RPV inlet to simulate forced flow coastdown. The coast-down of forced flow is simulated by varying the junction flow velocity linearly from the initial value to zero in a specified time period. The nominal coastdown period is 180 seconds. At the end of the coastdown, a valve is tripped open to provide a flow path between the PCU outlet and the downcomer of the reactor. The break is initiated at time zero of a transient case and the reactor is tripped on an upper plenum pressure of 6.0MPa. Reactor power after scram is calculated by the RELAP5 point-kinetics model and the fission product decay information specified is ANS79-1.

### **2.2.1 Transient Cases**

A series of transient analysis has been done to evaluate the effect of guard containment pressure on the passive mode of decay heat removal by natural circulation cooling. The effect of back pressure on natural circulation cooling of the pin core is evaluated by parametrically varying the free volume of the guard containment. The nominal case (Case 1) has an assumed guard

containment volume of 27000 m<sup>3</sup> and a final calculated pressure of 0.574MPa. The other cases have volumes and final pressures as shown below.

Case Identification	Guard Containment Free Volume (m <sup>3</sup> )	Final Containment Pressure (MPa)
Case 1	27000 (Nominal)	0.574
Case 2	0.5 x Nominal	0.901
Case 3	1.33 x Nominal	0.472
Case 4	0.75 x Nominal	0.675

Only two of the four cases resulted in an end state whereby natural circulation cooling has sufficient capacity to remove decay heat generated by the 2400 MW core. The results indicate that the guard containment back pressure has a dominant effect on the rate of heat removal by natural circulation with higher pressure leading to higher flow rate. Results of each parametric case and an analysis of the transient results for all four cases considered together are provided in the following sections.

### 2.2.1.1 Case 1

This case assumes the guard containment has a nominal free volume of 27000m<sup>3</sup>. Maximum fuel temperature in the hot channel exceeded 1600°C at about 14350s after initiation of the break (see Figure 2-12). At that time the pressures in the reactor and the guard containment have equilibrated to about 0.57MPa (see Figure 2-9).

### 2.2.1.2 Case 2

This case has a guard containment free volume of 13500 m<sup>3</sup> (half that of the nominal value). Pressures in the reactor and the guard containment converge to about 0.9MPa (see Figure 2-9) at the end of the calculation, 21600s after initiation of the break. The emergency heat exchanger is able to match the decay power (see Figure 2-7) and the maximum fuel temperature of 1274.4K is reached at 13540s (see Figure 2-12).

### 2.2.1.3 Case 3

This case assumes a guard containment volume of 36000 m<sup>3</sup>, a third larger than the nominal volume. The outcome is similar to Case 1. Maximum fuel temperature in the hot channel exceeded 1600°C at 13967s after initiation of the break (see Figure 2-12). At that time the pressures in the reactor and the guard containment have equilibrated to about 0.47MPa (see Figure 2-9).

#### 2.2.1.4 Case 4

This case has a guard containment free volume of 20250 m<sup>3</sup> (0.75 that of the nominal value). Pressures in the reactor and the guard containment converge to about 0.675MPa (see Figure 2-9) at the end of the calculation, 24000s after initiation of the break. The emergency heat exchanger is able to match the decay power (see Figure 2-7) and the maximum fuel temperature of 1736.9K is reached at about 22700s (see Figure 2-12).

### 2.2.2 Analysis of Transient Results

The general progression of the depressurization transient for the four parametric cases is very similar and the transient results for all four cases are plotted together to facilitate comparison of trends.

#### 2.2.2.1 Heat Removal Rate of the Emergency Cooling System

Plotted in Figure 2-7 is the rate of heat transfer into the water side of the HEATR1C heat exchanger. The plot shows the reactor power and the heat removal rate for four different cases (Case 1, Case 2, Case 3, and Case 4) over a period of 24,000 seconds. The reactor power starts at approximately 2.8e+08 W and decays to about 2e+07 W. The heat removal rate for all cases starts at a high value (around 1.5e+08 W) and decays to match the reactor power by approximately 10,000 seconds.

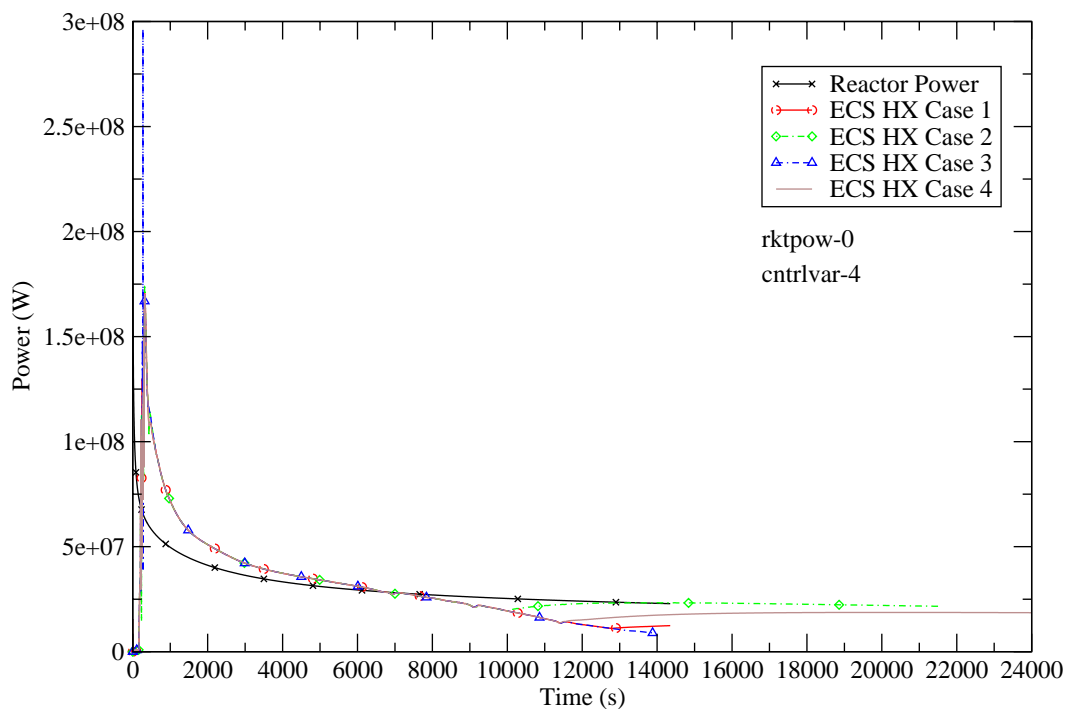


Figure 2-7 – Reactor power and Emergency Heat Exchanger heat removal rate.

The initial surge in the heat removal rate is due to the hydraulic transient on the water side of the heat exchanger (see Figure 2-15). A comparison between Figures 2-7, 2-8 and 2-9 shows that as the reactor pressure comes into equilibrium with the guard containment pressure, indicating an end to the depressurization phase of the transient, there is a slow migration of the heat exchanger heat removal rate towards the reactor power. This trend is indicative of the approach to a quasi-steady state where the natural circulation heat removal rate matches that of the reactor power.



### 2.2.2.2 Reactor Pressure

The pressure of the reactor upper plenum is shown in Figure 2-8. With the initiation of the break at time zero, the current RELAP5/ATHENA model assumes a linear coastdown of flow velocity from the power conversion unit (PCU) to the reactor. This is an interim scheme to simulate the behavior of a tripped PCU until a compressor/turbine model is developed for a more realistic representation of the PCU. The mean initial pressure of the PCU is less than the reactor pressure. With no rotating machinery in the current model to provide hydraulic head in the PCU, helium gas in the reactor quickly depressurizes into the PCU volumes. This results in a rapid drop in reactor pressure at time zero. The rest of the depressurization is more gradual and is due to leakage through the break into the guard containment. For much of the depressurization transient the helium flow through the leak is choked and thus all four parametric cases have similar reactor pressure until the point the reactor pressure equalizes with the guard containment pressure. In the two failed cases (Cases 1 and 3) the peak clad temperature exceeds the limit of 1600°C after the reactor pressure has dropped below 0.6MPa. If reliance on natural circulation cooling is delayed after a depressurization accident, e.g. by means of other active heat removal mechanisms such as battery powered pumps.

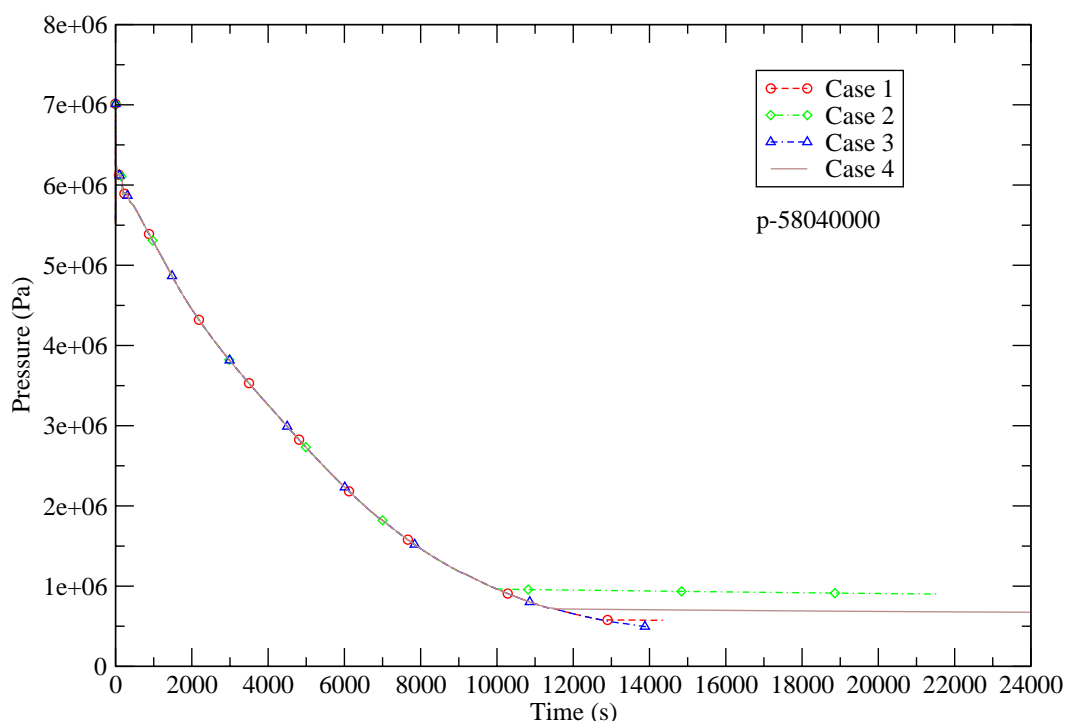


Figure 2-8 – Reactor pressure in the upper plenum.

### 2.2.2.3 Guard Containment Pressure

There are several factors that determine the pressure build up in the guard containment after a leak in the reactor primary circuit. They are:

1. Initial state of the guard containment atmosphere, i.e. temperature, pressure, and volume.

2. Presence of heat structure to absorb sensible heat inside the guard containment.
3. Presence of active cooling device in the guard containment.
4. Through wall heat transfer to the outside.
5. Energy and mass transfer through the leak into the guard containment.

In Figure 2-9 the rate of pressure build up is seen to vary inversely with the assumed free volume of the guard containment. A peak pressure is reached when the combined heat removal from the Emer decay

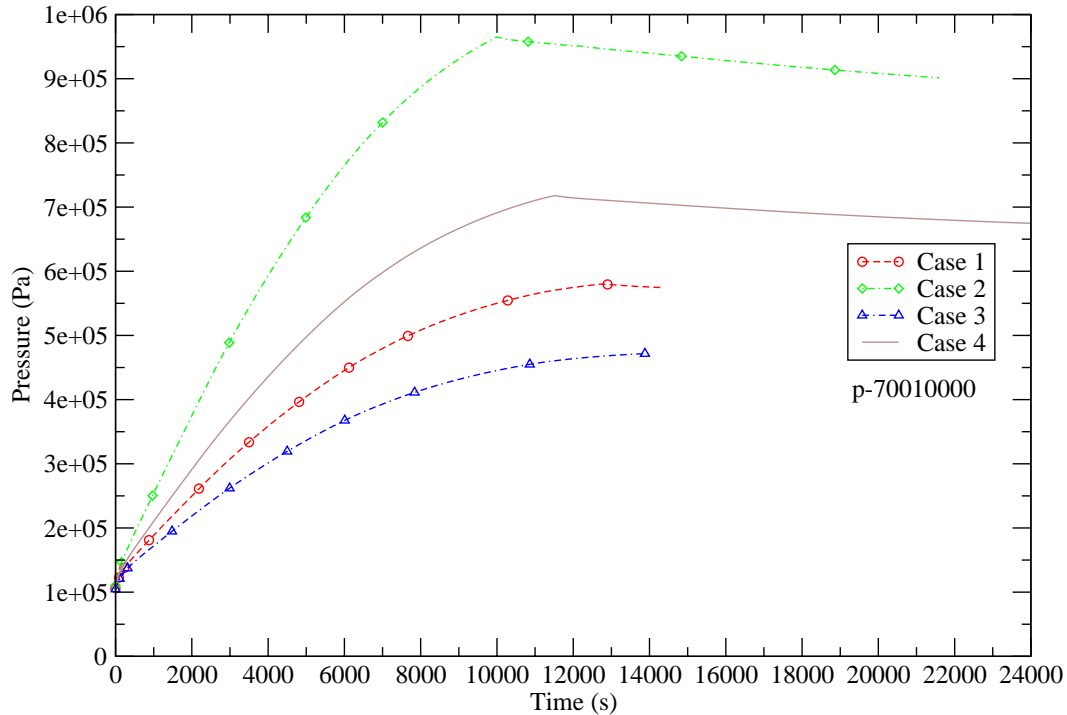


Figure 2-9 – Guard containment pressure.

It is noted that there are three means to mitigate the peak pressure inside the guard containment, by increasing the free volume, by vent the guard containment, and by using active heat removal. The viability of these means to minimize the peak pressure needs further evaluation.

#### 2.2.2.4 Guard Containment Gas Temperature

The gas temperature of the guard containment increases rapidly after the initiation of the depressurization accident because of the relatively low heat capacity of its atmosphere. Figure 2-10 shows that the peak gas temperature varies inversely with the free volume of the guard containment. A high gas temperature is of concern not only for the environmental qualification of equipment and instruments inside the guard containment but also for the structural integrity of the support structures and the guard containment itself.

### 2.2.2.5 Hot Assembly Fuel Temperature

The general trend of the temperature transient experienced by the fuel is discussed with the aid of Figure 2-11, which shows the average temperature of the fuel node of the hot assembly near top of the c cases. ]

s.

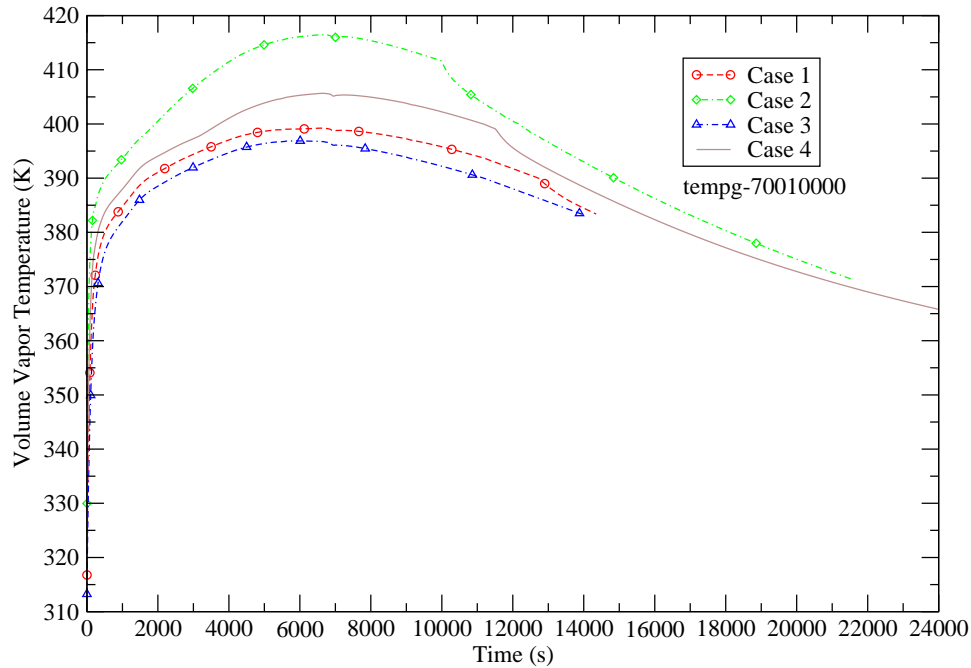


Figure 2-10 – Gas temperature inside the guard containment.

The initial drop in fuel temperature after the initiation of the transient is due to the rapid decrease in reactor power from operating level to decay heat level. The first temperature peak of slightly less than 1200K is from a combination of an increase in core inlet temperature (partly due to the approximate representation of the PCU in the current model) and a decrease in heat loss from the fuel when the flow from the PCU coasts down to zero. The duration of the coastdown has been found to be an important factor in deciding the magnitude of this first peak in fuel temperature. As natural circulation flow begins to develop through the core the rate of heat transfer from the fuel begins to increase again resulting in a decrease in fuel temperature. While the decay power is decreasing in time the natural circulation flow through the core is also slowing down because of loss in pressure through the leak. A minimum fuel temperature is reached at about 4000s into the transient and from that point on the fuel temperature begins an upward trend. With increasing fuel temperature the amount of heat transfer from the fuel into the flowing helium also increases. For the two success cases (Cases 2 and 4) the decay power eventually drops below the level that is sustainable by the helium flow and at a time before the fuel temperature limit is reached.

### 2.2.2.6 Maximum Fuel Temperature

Figure 2-12 shows the maximum fuel temperature as a function of time. It is obtained from the RELAP5/ATHENA results by defining a control variable that searches for the maximum

tempe  
tempe

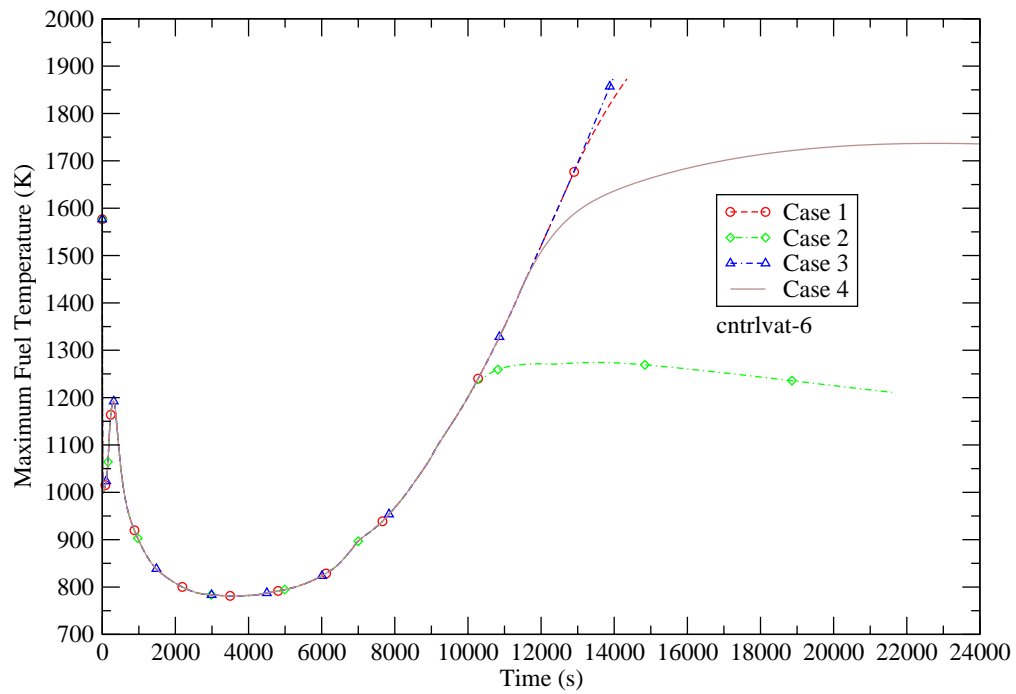
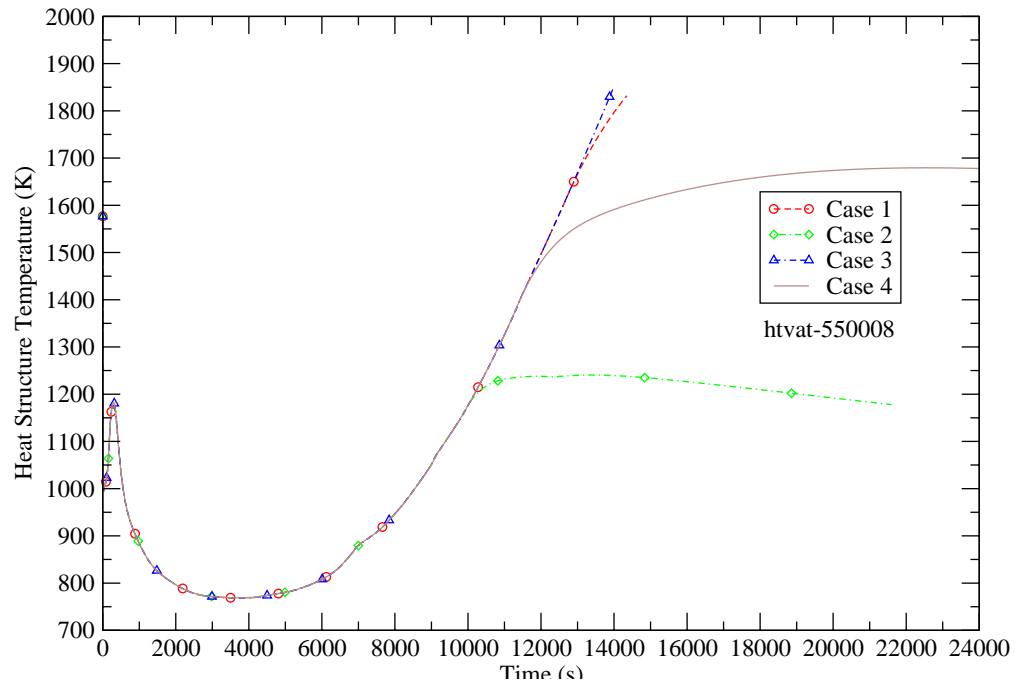


Figure 2-12 – Maximum fuel temperature core-wide.

### 2.2.2.7 Helium Flow in Natural Circulation

Natural circulation flow is established when the pressure difference across the check valve in the emergency heat exchanger loop has reached a threshold value. The helium flow rate shown in Figure 2-13 clearly demonstrates its dependence on the reactor pressure (see Figure 2-8). Higher flow rates are achieved at higher pressures. Based on economic and engineering constraints, the flow rate must be maintained at a minimum of 10 kg/s.

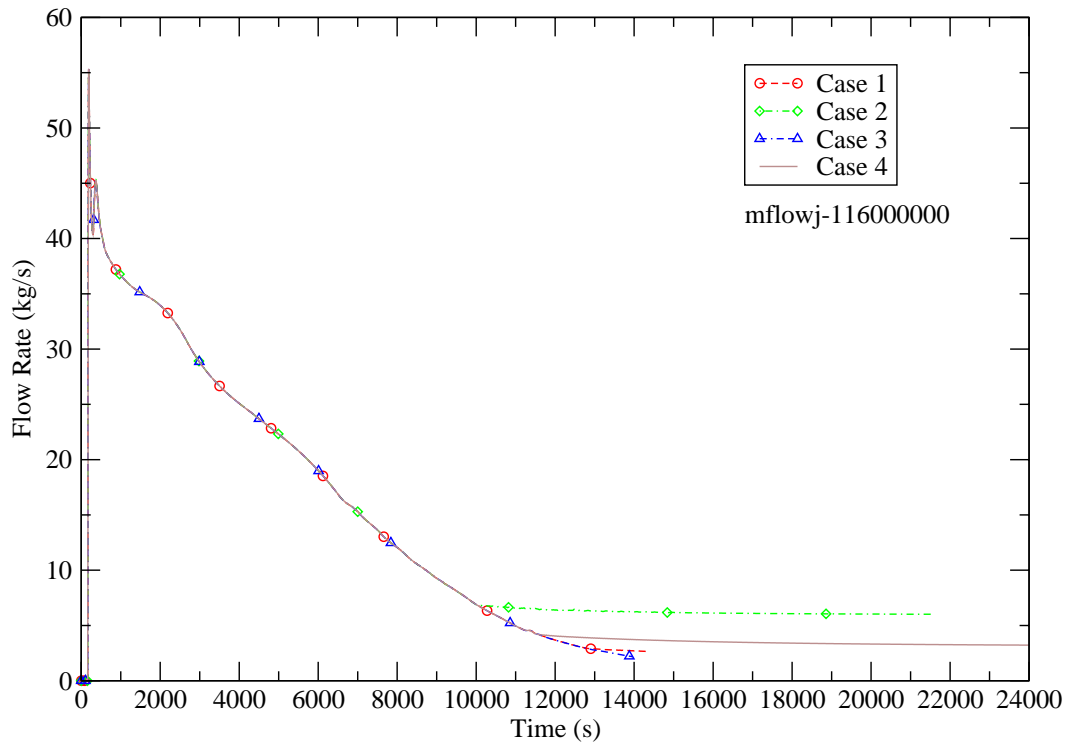


Figure 2-13 – Natural circulation flow rate of helium gas.

### 2.2.2.8 Gas Temperature at Core Outlet

The gas temperature at core outlet, shown in Figure 2-14, generally reflects the rate of heat transfer from the core to the helium flow. The progression of the core outlet temperature thus follows the trend of the fuel temperature shown in Figure 2-11.

### 2.2.2.9 Gas Temperature at Core Inlet

The initial surge in the core inlet temperature, shown in Figure 2-15, is somewhat unrealistic and is due to an approximation in the current PCU model discussed earlier in relation to the reactor pressure. In general the trend of the core inlet temperature corresponds to the difference between the heat removal rate of the emergency heat exchanger and reactor power. A positive differential implies a decrease in core inlet temperature and vice versa.

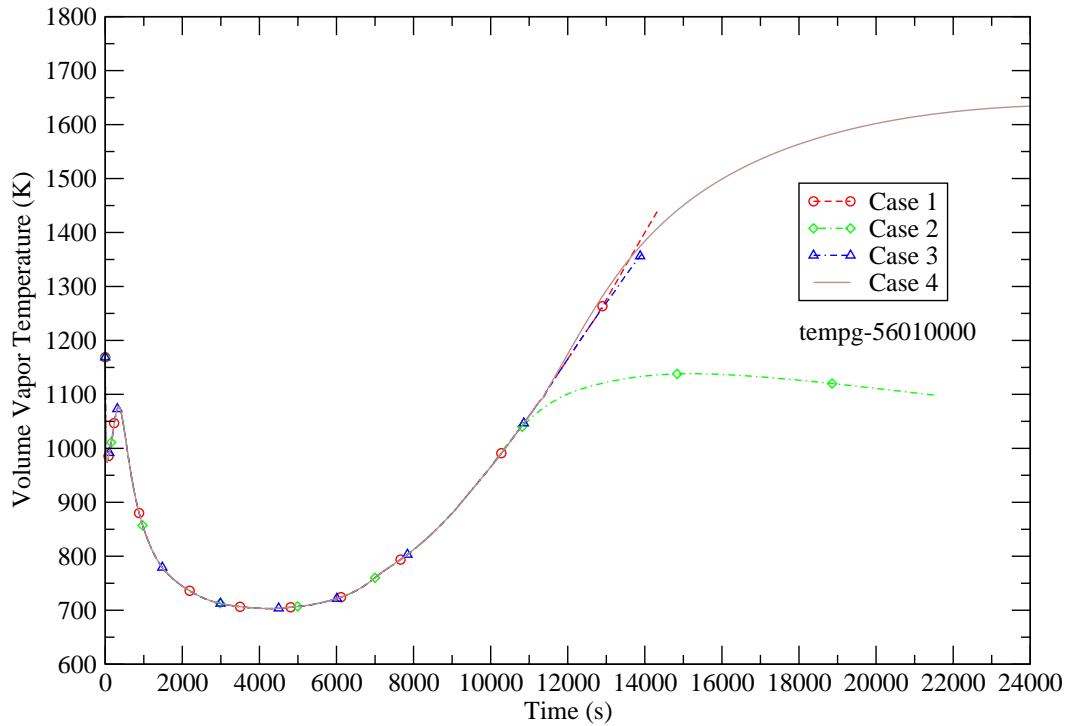


Figure 2-14 – Gas temperature at core outlet.

#### 2.2.2.10 Water Flow Rate in the HEATRIC Heat Exchanger

The dynamic behavior of the water flow on the secondary side of the HEATRIC heat exchanger is shown in Figure 2-16 for flow at the inlet. The water flow is initiated by the commencement of helium flow on the primary side of the heat exchanger following the opening of the check valve. Since the water is initially stagnant a sudden influx of heat into the water channel prompted steam generation in the flow channel. The generation and collapse of steam voids in the water circuit create oscillations in the water flow. Eventually a stable natural circulation flow is established on the secondary side of the HEATRIC heat exchanger. Since water is incompressible a surge volume is needed to accommodate the thermal expansion of the flowing water. The variation of water flow rate among the parametric cases is small. Nonetheless qualitatively the result shows a higher water flow rate corresponding to a lower core inlet temperature (see Figure 2-15).

#### 2.2.2.11 Water Temperature at the Outlet of the HEATRIC Heat Exchanger

The initial heat transfer to the water side is fairly high (see Figure 2-7) and this is reflected in the two-hundred-degree plus increase in the outlet temperature, as shown in Figure 2-17, a short time after flow has started in the heat exchanger. Changes in water temperature correspond to variations in the heat removal rate of heat exchanger. This indicates the operation of the secondary side is stable and follows the demand of the primary side.

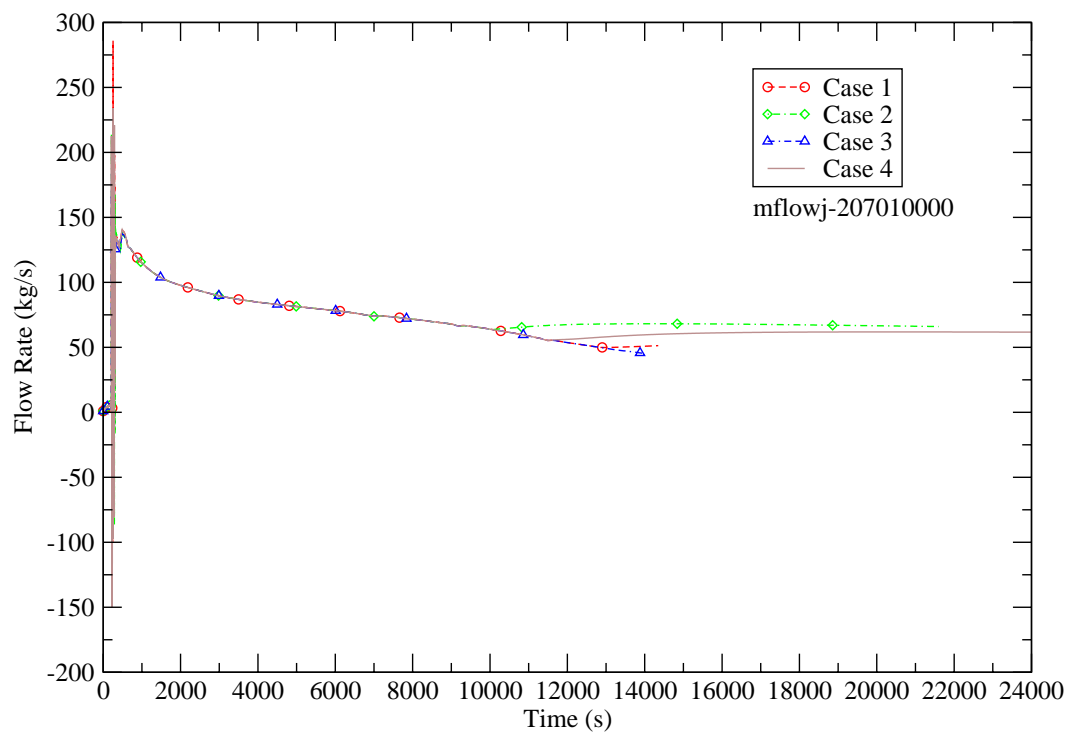
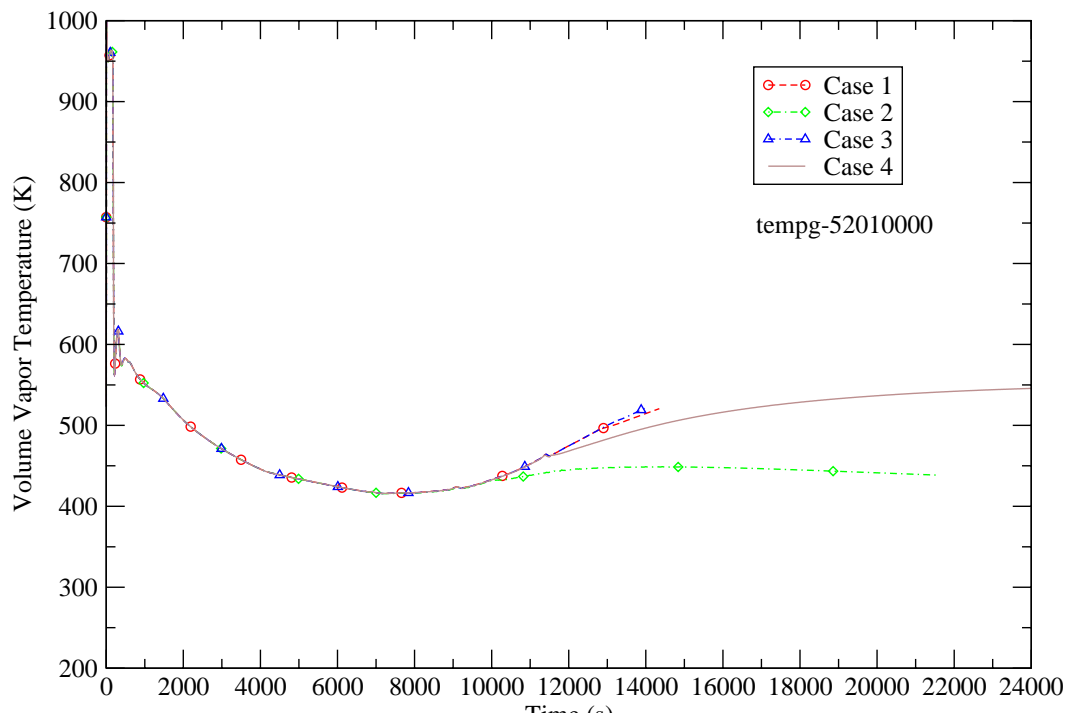


Figure 2-16 – Water flow rate in the HEATRIC heat exchanger.

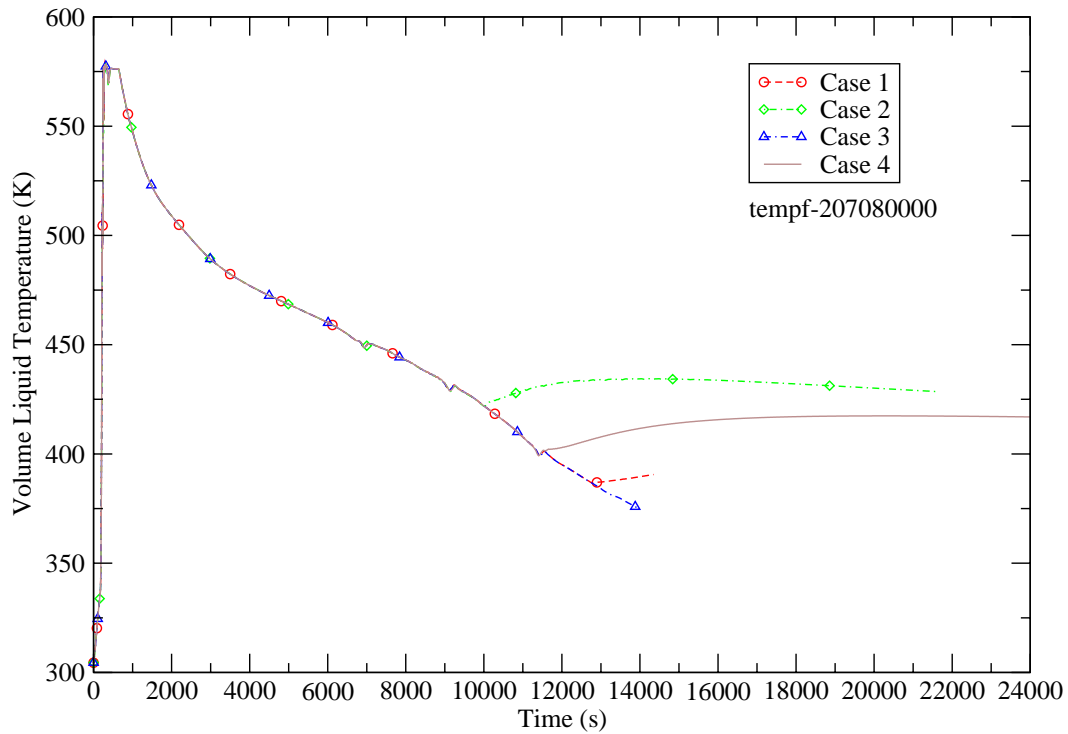


Figure 2-17 – Water temperature at the outlet of the HEATRIC heat exchanger.

### 2.2.2.12 Impact of Radiative Heat Transfer

The contribution of radiation heat transfer to the overall cooling of the fuel pins is demonstrated by the following tabulation that shows the energy balance for the upper half of the fuel pin in the hot assembly for Case 4 at the end of the calculation (24000s).

Heat Structure Node Number	Loss by Radiation (W)	Loss by Convection (W)	Power Source (W)	Net Loss of Power (W)
550006	12796	44351	56987	159.71
550007	14102	38994	52931	165.25
550008	11292	27168	38335	124.76
550009	6362	14334	20629	67.159

The heat structure temperatures and the coolant temperatures are shown below.



Heat Structure Node Number	Length of Node (m)	Fuel Temperature (K)	HEX Can Temperature (K)	Coolant Temperature (K)
550006	0.20205	1408.64	1378.97	1382.74
550007	0.20205	1567.93	1543.47	1546.71
550008	0.168381	1677.87	1658.29	1660.90
550009	0.101029	1735.77	1718.96	1721.17

The above tabulation shows that radiation accounts for 20-30% of the power loss from the fuel pin in the hot assembly. Radiation heat transfer becomes less significant for heat structures as their distance from the hot assembly is increased. The presence of unheated heat structures inside the reactor vessel increases the heat capacity of the system and this also helps to lower the heatup of the helium gas inside the vessel.

### **2.3 Summary and Conclusions**

The analysis of depressurization transient reported here for the 2400MW pin core design is an extension of an earlier analysis [2-4] for a 600MW core with half the power density of the current design (50W/cc versus the current 100W/cc). Major differences between the earlier analysis and the current one are in the fuel pin dimensions, the core power distribution, and the design of the emergency cooling system. In particular, the emergency heat exchangers are now located ex-vessel and compressed water is used as the working fluid on the secondary side. In addition, radiation heat transfer is included in the current analysis.

The following conclusions can be drawn from this preliminary study:

- 1) With a 100W/cc core power density the sensitivity of maximum fuel temperature to core power distribution has pointed to the need of a more uniform core power distribution radially and axially.
- 2) Fuel pin design (pellet size, gap and clad thickness) also has a significant impact on the fuel temperature response in a depressurization accident.
- 3) In order to maintain the maximum fuel temperature within acceptable limits, the guard containment pressure must be at least  $\sim 0.675$  MPa. This pressure implies that the free volume of the guard containment can be no greater than  $20,250 \text{ m}^3$ .
- 4) Heat structures and radiative heat transfer are important phenomena in the post-accident thermal progression of the core. The effect of including these phenomena is to re-distribute the radial temperature profile compared to not including them. Briefly, the hot zones (fuel) are reduced in temperature, and the cold zones (reflector, shield etc.) are increased in temperature relative to not including the above mentioned phenomena.
- 5) The coolant flow due to the coast down of the Turbine-Compressor-Generator (TCG) unit is an important factor in initially cooling the core following reactor scram, and in establishing the natural circulation flow. Currently this flow is approximated by linearly reducing the flow velocity to zero in 180 seconds. A more realistic model of this flow reduction (both mass

flow rate and time) is required to make more accurate estimates of the maximum fuel temperature, and ultimately the guard containment volume. In order to carry out this more realistic calculation, a complete Turbine Compressor model is required. This model will require the appropriate performance maps, inertia of the rotating parts, and some estimate of the internal friction of the blades rotating in the working fluid.

- 6) The emergency heat exchanger needs to be orientated in a vertical direction rather than horizontally, to avoid boiling of the pressurized water on the secondary side. The hot helium initially leaving the core causes the water on the secondary side to boil in the case of a horizontally orientated heat exchanger. This boiling induces flow oscillations, and potentially reverse flow on the secondary side, impeding the onset of natural circulation flow. These events are minimized in the case where the heat exchanger is oriented vertically, and the start of natural circulation flow proceeds smoothly.
- 7) Helium flow caused by either coast down or normal operation using emergency power supply (battery) of the ECS blower is not included in this calculation. This additional flow will help in establishing the natural circulation flow pattern following the start of the accident and also reduce the requirement of natural circulation cooling by prolonging the period of forced flow cooling. However, natural circulation flow is established in the current analysis, despite not including this flow. Thus, it would seem that including this flow is not crucial to cooling the core but its inclusion is necessary to create an accurate model of the accident progression.

## **2.4 References**

- [2-1] "ATHENA Code Manual Volume I: Code Structure, System Models and Solution Methods," INEEL-EXT-98-00834, Revision 2.2, October 2003.
- [2-2] Feldman, E. and Wei, T., "GFR Pin Core Designs for Passive Decay Heat Safety," I-NERI Project #2001-002-F Report GFR022, February, 2004.
- [2-3] Personal Communication with Tom Wei of ANL, December 6, 2004.
- [2-4] Cheng, L. and Ludewig, H., "Passive Decay Heat Removal Transient Analysis for Pin Core," I-NERI Project #2001-002-F Report GFR015, February, 2004.

### 3. Effects of the Reactor Cavity Cooling System

The ATHENA analysis presented here examines the effects of the reactor cavity cooling system (RCCS) on decay heat removal for a gas-cooled reactor during a depressurization accident. The new analysis is an extension of a previous study [3-1] that assessed the performance of decay heat removal by natural circulation cooling under a depressurization accident for a helium-cooled reactor. In the previous analysis passive decay heat removal is enabled by an emergency cooling system (ECS) that directs by natural circulation the hot helium gas from the reactor to an ex-vessel heat exchanger. A dominant factor in determining the effectiveness of natural circulation cooling is the system pressure. A higher pressure results in a denser gas and that leads to a higher buoyancy head and subsequently a higher flow rate. In a depressurization accident initiated by a component breach the pressures of the reactor vessel and the guard containment will converge to an intermediate value. The impact of this common pressure on the maximum fuel temperature has been evaluated parametrically in the previous study. In that analysis different common pressures (system back pressure) were realized by varying the free volume of the guard containment. An alternate means of decay heat removal is the RCCS that surrounds the reactor vessel. Core decay heat is transferred to the reactor vessel by conduction and radiation and the RCCS absorbs the thermal energy from the reactor vessel directly by radiation and indirectly from the guard containment atmosphere by convection. The impact of the RCCS on the guard containment atmosphere and the maximum fuel temperature is the subject of the present study.

#### 3.1 ATHENA/RELAP5 Model

In the current analysis heat structures and hydraulic volumes are added to represent the RCCS and the new system replaces the heat structure in the previous model that represented the reactor vessel support structure. The heat structures used in the ATHENA model for convective and radiative heat transfers are shown in Figure 3-1.

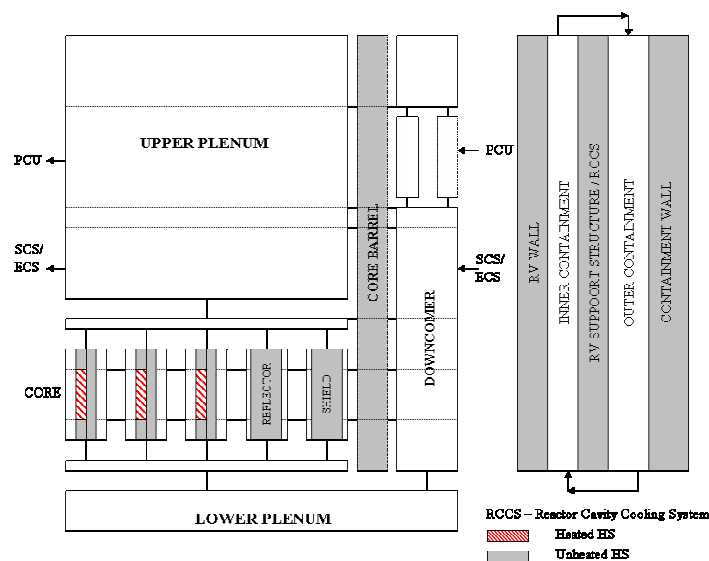


Figure 3-1 – Reactor Vessel and Guard Containment Heat Structures.

The heated heat structures (HS), i.e. the fuel pins, identified in Figure 3-1 is the source of energy and the unheated heat structures are other components that participate in the exchange of thermal energy by radiation. In the previous analysis [3-1] the zone of influence of radiative heat transfer is assumed to be confined to the cylindrical section that coincides with the vertical extent of the fueled region of the core. As an example, though the core barrel (also, the reactor vessel wall, and the reactor vessel support structure) extends to the upper plenum, only the lower portion between the lower and upper boundaries of the fueled zone (1.347m in height) participates in radiative heat transfer. This assumption is relaxed in the current analysis to accommodate the RCCS that spans the entire height of the reactor vessel. In particular the entire core barrel now communicates radiatively with the full height of the reactor vessel wall and in turn the full height of the reactor vessel radiates to either the vessel support structure (old configuration) or the RCCS (new configuration).

The ATHENA model for the RCCS is based on a set of input developed at INL [3-2]. As shown in Figure 3-2 the RCCS is modeled with three cylindrical heat structures that are concentric with the reactor vessel. The inner wall (HS 9700), closest to the reactor vessel is followed by the interior wall (HS 9701) and the outer wall (HS 9600) respectively. The incoming (down flow) and outgoing (up flow) streams of cooling water are separated by the interior wall.

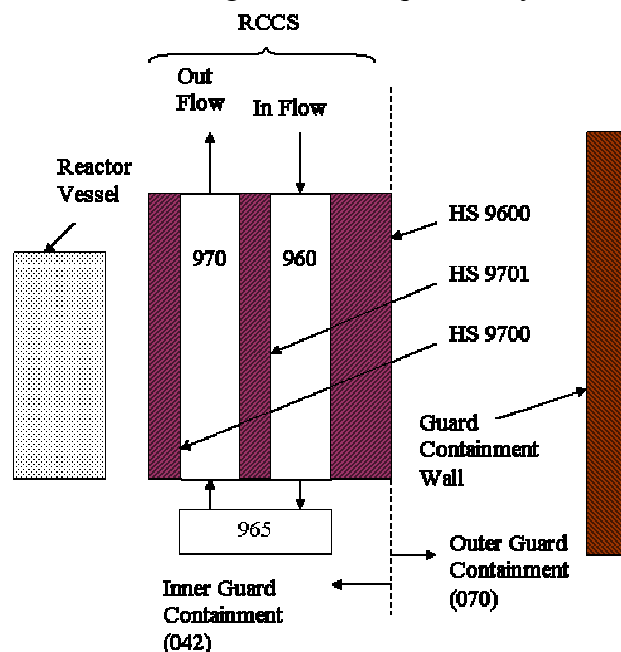


Figure 3-2 - ATHENA Model of the RCCS

The inner wall is made of stainless steel and has a wall thickness of 0.0127m. This wall is in contact with the inner guard containment volume (042) that occupies the part of the guard containment that is within the confine of the RCCS and also includes the region above the reactor and the RCCS. The interior wall of the RCCS is modeled with a 0.01746m of low conductivity material. The outer wall of the RCCS has two layers, a 0.0127m of stainless steel and a 1m thick wall of concrete. The concrete wall is in contact with the atmosphere of the outer guard containment volume (070). The inner and outer guard containment volumes are connected

at the top and bottom to facilitate internal recirculation. The wall of the 44m high guard containment is modeled with a 0.02m concrete wall.

It is assumed in the ATHENA calculations that the outside surface of the guard containment wall is kept at a constant temperature of 30°C by a thermal management system embedded in the wall. The RCCS is assumed to be cooled by 30°C water and the flow is high enough to maintain the temperature rise to less than 1 deg. C. These two boundary conditions are set to maximize the cooling of the guard containment atmosphere by the containment wall and the RCCS.

### 3.2 ATHENA Transient Analysis

The new analysis with the addition of the RCCS is performed by using the same system model and the same depressurization accident as described in Ref [3-1]. With the modifications to the radiative heat transfer model for the core barrel, vessel wall, and vessel support structure, it becomes necessary to establish a new baseline analysis for use in comparison with the case of the RCCS. The new baseline case is similar to Case 4 described in Ref [3-1]. The depressurization accident is initiated by a 0.00645 m<sup>2</sup> (1.0 in<sup>2</sup>) rupture in the cold leg of one of the PCUs (4 loops of 600MW each). A guard containment free volume of 20250 m<sup>3</sup> is assumed and the initial pressure and temperature of the guard containment atmosphere are one atmosphere and 30°C respectively.

#### 3.2.1 Transient Cases

Two transient cases have been run, one with and one without the RCCS. The later is the new base case. The benefits of having the RCCS are evident in the guard containment conditions. Both the pressure and temperature of the guard containment are lower in the case with RCCS (Case 5) than the case without (Case 4a, the base case) it. The trend of lower temperature however does not extend to the peak fuel temperature Results of the two cases, at the end of a 24000s run, are summarized below.

Case Identification	Final Peak Fuel Temperature (K)	Final Containment Pressure (MPa)	Final Containment Temperature (K)
Case 4a (No RCCS, Base Case)	1594	0.658	355.
Case 5 (With RCCS)	1772	0.611	325.

It is noted that the maximum fuel temperature during the depressurization accident is only a few degrees from the final peak fuel temperature shown in the above table. With a lower guard containment pressure, the natural circulation flow established in the reactor is correspondingly lower in the case with RCCS. This then leads to a higher peak fuel temperature in Case 5. The result of the peak fuel temperature demonstrates that the predominant mode of decay heat removal is by convection while radiative heat transfer only serves a minor role in heat dissipation from the fuel. For the purpose of comparison, at the initial steady-state reactor power of

2400MW, the RCCS removes about 2MW of power while the emergency cooling system (ECS) removes about 20MW of power from the reactor at the end of the calculation at 24000s.

It is noted that though Case 4a is the same transient as Case 4 in Ref. [3-1], the new analysis has a few modifications in the inputs for the heat structures. These changes resulted in a generally lower guard containment pressure and lower temperatures (fuel and guard containment) than before.

### 3.2.2 Analysis of Transient Results

The progression of the depressurization transient for the two cases is very similar and the transient results for both cases are plotted together to facilitate comparison of trends.

#### 3.2.2.1 Heat Removal Rate of the Emergency Cooling System

Plotted in Figure 3-3 is the rate of heat transfer into the water side of the HEATRIC heat exchanger in the emergency cooling system. The reactor power also is shown in the figure for comparison. The initial surge in the heat removal rate is due to the hydraulic transient on the water side of the heat exchanger as explained in Ref. 1. A comparison between Figures 3, 4 and 5 shows that as the reactor pressure comes into equilibrium with the guard containment pressure, indicating an end to the depressurization phase of the transient, there is a slow migration of the heat exchanger heat removal rate towards the reactor power. This trend is indicative of the approach to a quasi-steady state that of the reactor power.

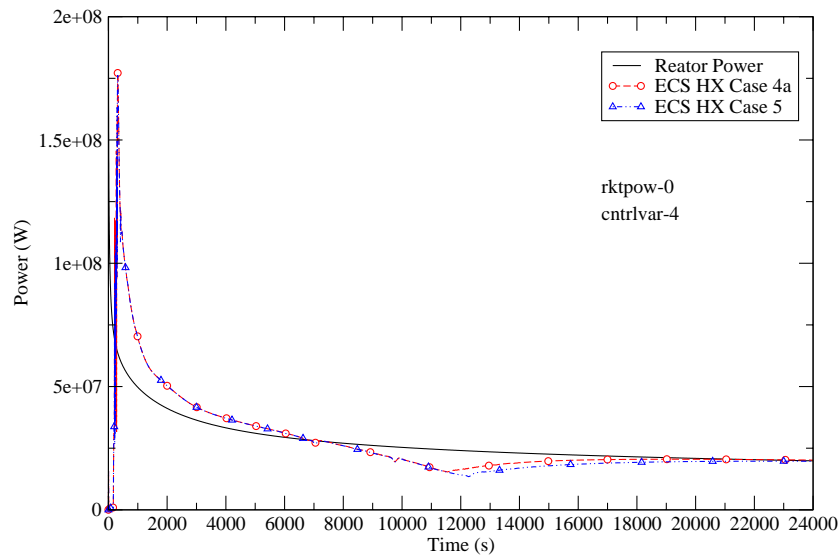


Figure 3-3 – Reactor Power and Emergency Heat Exchanger Heat Removal Rate.

#### 3.2.2.2 Reactor Pressure

The pressure of the reactor upper plenum is shown in Figure 3-4. With the initiation of the break at time zero, the current RELAP5/ATHENA model assumes a linear coast down of flow velocity from the power conversion unit (PCU) to the reactor. This is an interim scheme to simulate the behavior of a tripped PCU until a compressor/turbine model is developed for a more realistic

representation of the PCU. The mean initial pressure of the PCU is less than the reactor pressure. With no rotating machinery in the current model to provide hydraulic head in the PCU, helium gas in the reactor quickly depressurizes into the PCU volumes. This results in a rapid drop in reactor pressure at time zero. The rest of the depressurization is more gradual and is due to leakage through the break into the guard containment. For much of the depressurization transient the helium flow through the leak is choked and thus both cases have similar reactor pressure until the point at which the reactor pressure equalizes with the guard containment pressure. It is noted that the blowdown pressure in the reactor is approximately 7.1e+06 Pa. The reactor pressure in the

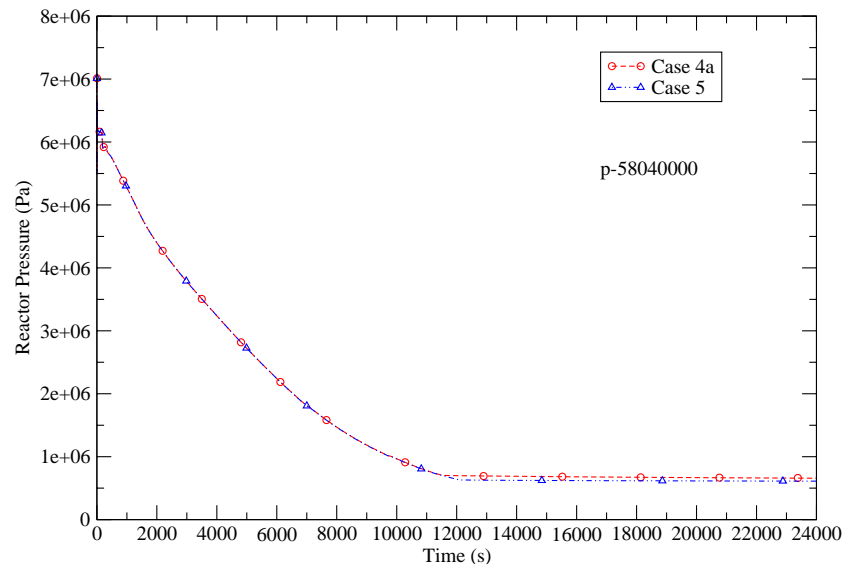


Figure 3-4 – Reactor Pressure in the Upper Plenum.

### 3.2.2.3 Guard Containment Pressure

There are several factors that determine the pressure build up in the guard containment after a leak in the reactor primary circuit. They are:

1. Initial state of the guard containment atmosphere, i.e. temperature, pressure, and volume.
2. Presence of heat structure to absorb sensible heat inside the guard containment.
3. Presence of active cooling device in the guard containment.
4. Through wall heat transfer to the outside.
5. Energy and mass transfer through the leak into the guard containment.

In Figure 3-5 the rate of pressure build up is seen to be faster for Case 4a than Case 5 and the former also has a higher containment pressure. A peak pressure is reached when the reactor and guard containment have reached the same pressure and the combined heat removal from the Emergency Cooling System, Reactor Cavity Cooling System, and heat conduction through the guard containment wall exceeds the decay power.

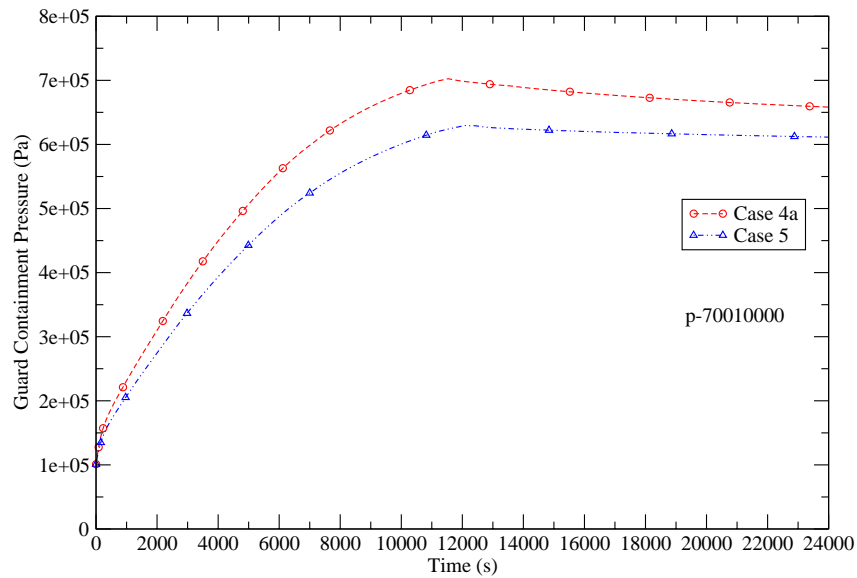


Figure 3-5 – Guard Containment Pressure.

### 3.2.2.4 Guard Containment Gas Temperature

The gas temperature of the guard containment increases rapidly after the initiation of the depressurization accident because of the relatively low heat capacity of its atmosphere. Figure 3-6 shows that the gas temperature is lower when the RCCS is included in the analysis. A high gas temperature is of concern not only for the environmental qualification of equipment and instruments inside the guard containment but also for the structural integrity of the support structures and the guard containment itself.

### 3.2.2.5 Peak Fuel Temperature

Figure 3-7 shows the peak fuel temperature as a function of time. It is obtained from the RELAP5/ATHENA results by defining a control variable that searches for the maximum temperature for all fuel heat structures at all axial locations. It is noted that there is little deviation between the peak fuel temperatures for the two cases until about 12000s when Case 4 has finished its blow down. Before that time the two cases have the same reactor pressure and almost the same natural circulation flow (see Figure 3-8). In both cases the maximum fuel temperature during the transient is within the success criterion of 1873K, with the RCCS case (Case 5) exhibiting a closer approach to the limit.



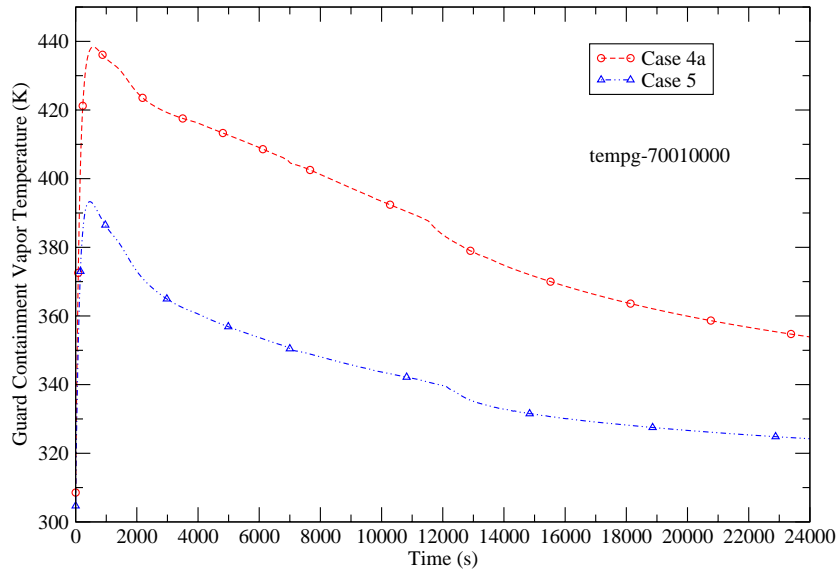


Figure 3-6 – Guard Containment Vapor Temperature Core-wide.

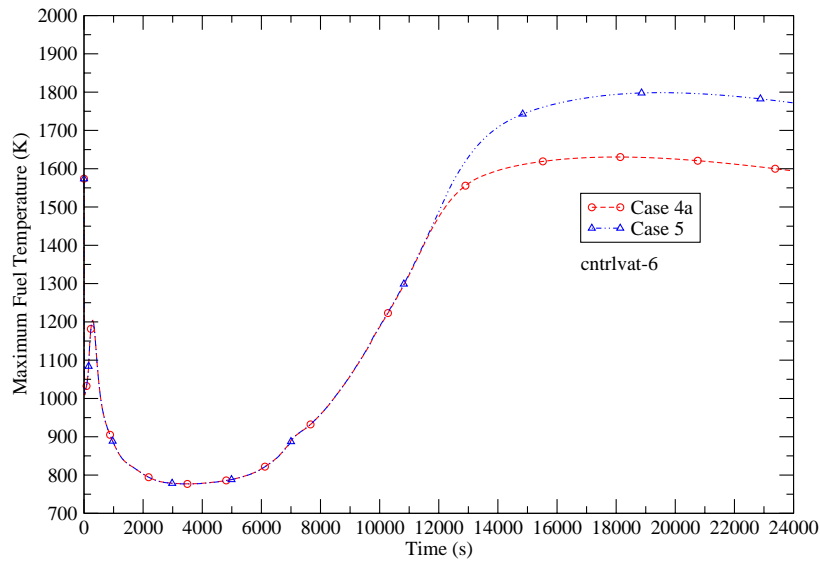


Figure 3-7 – Peak Fuel Temperature Core-wide.

### 3.2.2.6 Helium Flow in Natural Circulation

Natural circulation flow is established when the pressure difference across the check valve in the emergency heat exchanger loop has reached a threshold value. The helium flow rate shown in Figure 3-8 clearly demonstrates its dependence on the reactor pressure (see Figure 3-4). Higher flow rates are achieved at higher pressures and that is the reason for the base case to have a higher flow rate than the RCCS case when the system pressure has reached its quasi-steady state value. Based on economic and engineering constraints a maximum design pressure will be specified for the guard containment and that will have a direct bearing on the maximum passive heat removal rate achievable by natural circulation alone.

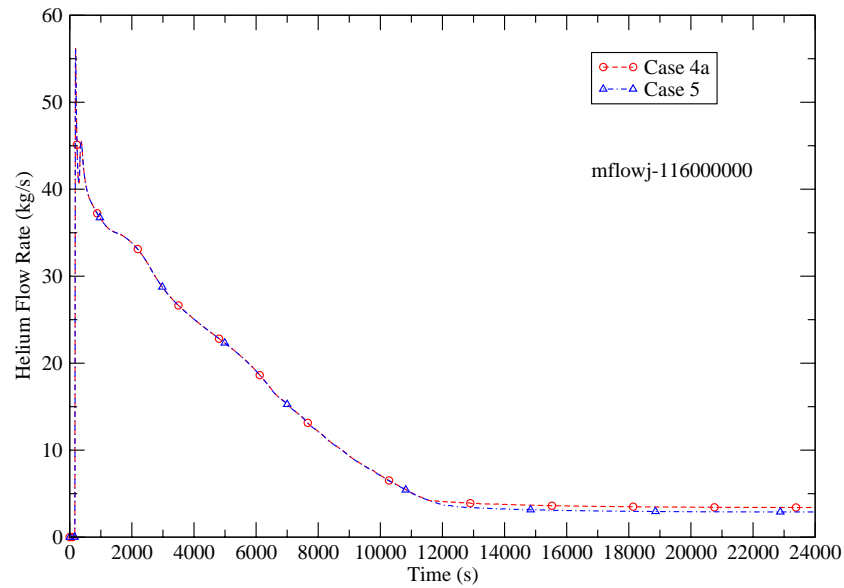


Figure 3-8 – Natural circulation flow rate of helium gas.

### 3.2.2.7 Gas Temperature at Core Outlet

The initial surge in the core inlet temperature, shown in Figure 3-10, is somewhat unrealistic and is due to an approximation in the current PCU model discussed earlier in relation to the reactor pressure. In general the trend of the core inlet temperature corresponds to the difference between the heat removal rate of the emergency heat exchanger and reactor power. A positive differential implies a decrease in core inlet temperature and vice versa. The core inlet temperature is very similar for both cases, with Case 4a showing a slightly higher initial surge. The core inlet temperature is shown in Figure 3-10.

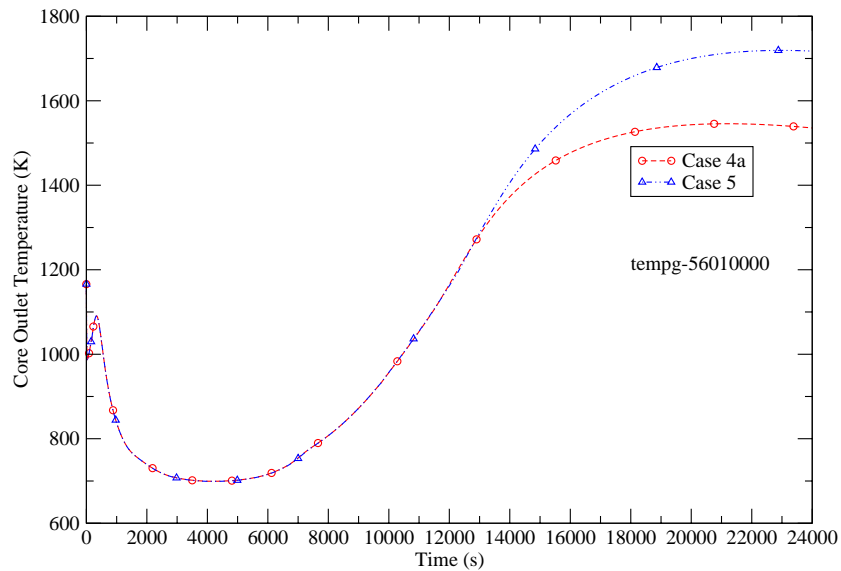


Figure 3-9 – Gas temperature at core outlet.

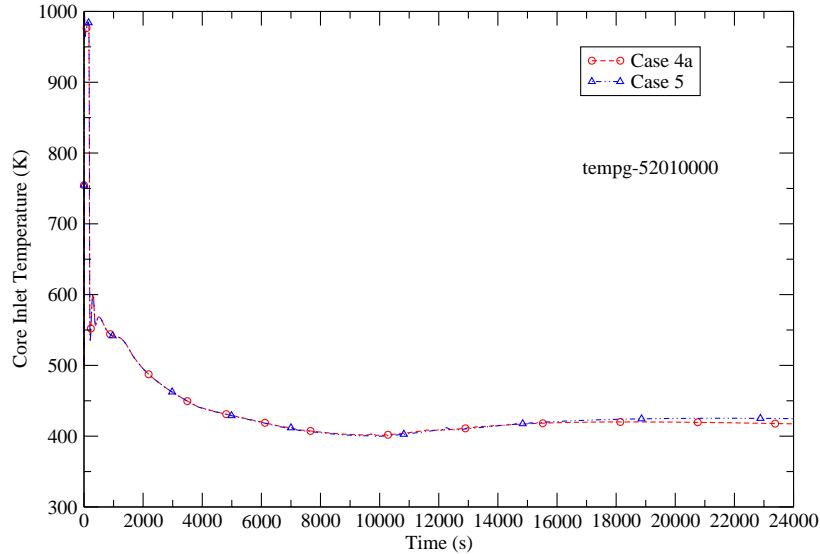


Figure 3-10 – Gas temperature at core inlet.

### 3.3 Summary and Conclusions

The analysis presented here is an extension of Section 2 of this report (and can be found in [3-1]) of a depressurization transient for a 2400MW gas cooled reactor with a passive decay heat removal scheme based on natural circulation cooling. This new analysis includes the effects of a Reactor Cavity Cooling System that surrounds the reactor. The analysis shows that while the RCCS is good for lowering the guard containment pressure and temperature, its presence has a negative impact on the peak fuel temperature because the lower back pressure also reduces the natural circulation flow that removes most of the decay heat by convection. While the RCCS may be beneficial for other non-LOCA type accidents, its use in a depressurization accident would require further studies to evaluate the trade-offs. The same observation applies to other active or passive means of cooling the guard containment atmosphere. One example is the heat loss through the guard containment wall. Internal flow inside the guard containment tends to be quite complex and to correctly model the loss of heat by convection to the wall would require a more detailed analysis than what is possible with a system code. The capability to accommodate other break sizes should also be evaluated in the design of the guard containment. It is also recognized that the accident analysis will not be complete without the power conversion unit being properly modeled.

### 3.4 References

- [3-1] Cheng, L., Ludewig, H. and Jo, J., “Passive Decay Heat Removal for a 2400 MW Pin Core by Natural Circulation,” BNL report submitted to the DOE GEN-IV Program, January 2005.
- [3-2] Davis, C., Personal communication with L. Cheng (Electronic files related to major improvements made to the RELAP5-3D/ATHENA computer code for analysis of the GFR as part of an annual report (2004) for an INL LDRD), April 7, 2005.

## 4. Modeling of the Power Conversion Unit (PCU)

As part of the system design and safety analysis of a direct-cycle gas cooled fast reactor (GCFR) ATHENA calculations [4-1,4-2] have been done to study passive decay heat removal by natural circulation cooling in the case of a depressurization accident. It has been recognized from the results of initial analyses that the coolant flow due to the coast down of the turbomachinery of the power conversion unit (PCU) is an important factor in initially cooling the core following reactor scram, and in establishing the natural circulation flow. Currently this flow is approximated by linearly reducing the flow velocity to zero in 180 seconds. A more realistic model of this flow reduction (both mass flow rate and time) is required to make more accurate estimates of the maximum fuel temperature, and ultimately the guard containment volume. In order to carry out this more realistic calculation a complete PCU model is required. This interim report discusses progress made in the detail modeling of the PCU that will become part of the ATHENA model of the GFR plant system.

### 4.1 GT-MHR Power Conversion Unit

The power conversion unit (PCU) of interest is a design that is being developed by General Atomics (GA) and its Russian partner for a 600 MWt Gas Turbine-Modular Helium Reactor (GT-MHR). Conceptual design of the GT-MHR was done by GA [4-3], and further development is being carried out in Russian with support from the US government [4-4]. A PCU has two major parts, the turbomachinery and the heat exchangers. A node diagram showing the gas volumes in a PCU is shown in Figure 4-1.

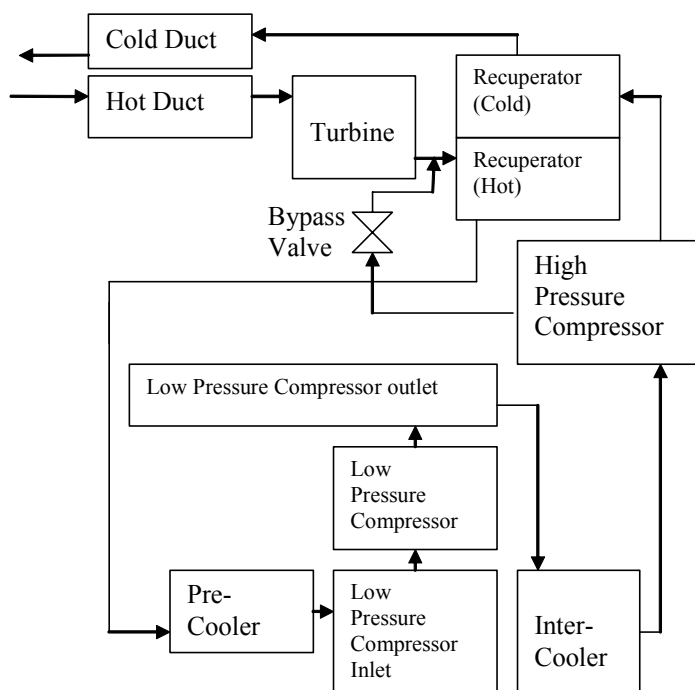


Figure 4-1 – Node Diagram of Power Conversion Unit.

The components of a PCU are housed in a vertical vessel that is placed near the reactor. The PCU and the reactor are connected by a short cross vessel that is made up of an inner hot duct and a concentric outer cold duct. Components of the turbomachinery, namely, the generator, turbine, low and high pressure compressors, are all on one shaft. The heat exchangers consist of recuperator, precoolers, and intercoolers. A bypass valve that connects the high and low pressure side of the PCU is used for the over-speed protection of the turbine. Geometric data for the various gas volumes in the PCU are from Ref. [4-5] and they are summarized in Table 4-1.

Table 4-1 - Geometric Data for a 600 MWt PCU

Component	Length (m)	Volume (m <sup>3</sup> )	Area (m <sup>2</sup> )	Orientation (Degree)	Hydraulic Diameter (m)
Hot Duct	7.4	11.885	1.606	0	1.43
Turbine	4.2	2.04	0.4857	90	0.7864
Turb - Recu	1.3848	0.6924	0.5	-90	0.7979
Recuperator-LP*	2.8152	59.5	21.135	-90	???
Recu - Prec	10.95	5.475	0.5	-90	0.7979
Precooler	4.73	134.48	28.431	-90	0.009924
LPC duct	4.9	11.786	2.405	90	1.75
LPC inlet	2.38	14.239	5.983	90	2.76
LPC	4.2	2	0.4762	90	0.7787
LPC outlet	4.9	21.3	4.347	-90	2.353
Intercooler	4.73	134.08	28.346	-90	0.009924
Intc - HPC	9.63	4.815	0.5	90	0.7979
HPC	4.2	2	0.4762	90	0.7787
HPC-Recu	2	1	0.5	0	0.7979
Recuperator-HP**	2.8152	59.5	21.135	90	???
Recu - Cduct	2.8152	1.4076	0.5	-90	0.7979
Cold Duct	7.4	13.949	1.8850	0	0.6
Total Volume		480.15			

\* LP = low pressure side of recuperator.

\*\* HP = high pressure side of recuperator.

Stand-alone ATHENA models of the turbine, compressors, recuperator, precoolers, and intercoolers have been prepared. In general the predicted thermal capacities of the components are within a few percent of the values shown in Table 4-2.

## 4.2 Helium Brayton Cycle

The thermal cycle utilized in a GT-MHR plant is a recuperative gas turbine cycle with intermediate cooling. Helium from the reactor enters the PCU via the hot gas duct inside the cross vessel and expands in the gas turbine. The turbine drives the rotor of the generator and the two compressors (low and high pressure). After the turbine, the helium returns much of the remaining thermal energy back to the cycle via a high efficiency recuperator. A precoolers removes heat from the helium to the ultimate heat sink when the gas emerges from the low pressure side of the recuperator. Then a low pressure compressor pressurizes the gas before an intermediate cooler removes more heat from the helium. A high pressure compressor raises the helium pressure before the gas comes into the high pressure side of the recuperator. From there the helium flows to the reactor via the annular space between the hot duct and the wall of the

cross vessel. In the reactor, the helium gas passes through the core and closes the Brayton cycle. The state points of the helium at various stages of the cycle are summarized in Table 2 [4-5, 4-6]. The thermal capacity shown in the table is based on information from Ref. [4-7].

Table 4-2 – Helium State Points

Component	Inlet Conditions	Outlet Conditions	Thermal Capacity
Turbine	848 °C 7.07 MPa	508 °C 2.61 MPa	558.5 MW
Recuperator (Low Pressure)	508 °C 2.61 MPa	130.3 °C 2.58 MPa	639 MW
Precooler	130.3 °C 2.58 MPa	26.4 °C 2.55 MPa	173 MW
Low Pressure Compressor	26.4 °C 2.55 MPa	107.5 °C 4.31 MPa	132.3 MW
Intercooler	107.5 °C 4.31 MPa	26 °C 4.28 MPa	130.2 MW
High Pressure Compressor	26 °C 4.28 MPa	110.3 °C 7.24 MPa	134.5 MW
Recuperator (High Pressure)	110.3 °C 7.24 MPa	488 °C 7.16 MPa	639 MW

### **4.3 Turbomachinery**

The primary components of the turbomachinery consist of the generator, the turbine, and the low and high pressure compressors. The rotating parts are all mounted vertically on one shaft. Some of the mechanical characteristics of the turbomachinery, such as mass, size, and capacity are summarized in Ref. [4-8].

#### **4.3.1 Turbine**

Since the performance data for the multi-stage turbine is not available only an approximate ATHENA model is used to represent the gas turbine. It is modeled as a single stage type 2 turbine, i.e. constant efficient stage.

#### **4.3.2 Low and High Pressure Compressors**

Again only approximate models are used to represent the compressors. The pump model is used as a surrogate for the compressor because the released version of ATHENA (ver. 2.2.4) did not have the compressor model yet. Had the compressor model been available the lack of performance characteristics for the compressors would still make the construction of an ATHENA model for the GT-MHR compressors difficult.

### **4.4 Heat Exchanger**

Located in the annular space between the turbine-compressors and the PCU vessel is the recuperator, the precooler and the intercooler. The coolers are cooled by running water that transfers heat to the ultimate heat sink.

#### **4.4.1 Recuperator**

Helium gas, to and from the reactor, flow on opposite side of the recuperator. The recuperator is a vertical modular heat exchanger with plate-fin heat transfer surface and operating with countercurrent flow [4-7, 4-8, 4-9, and 4-10]. The heat transfer coefficient calculated by ATHENA for a flat plate is adjusted by using the fouling factor input to achieve the desired heat transfer rate for a given flow and surface area.

#### **4.4.2 Precooler and Intercooler**

The precooler and the intercooler have similar design [4-7, 4-8, and 4-11]. They are both modular vertical heat exchangers. Each module consists of a number of straight tubes with outer fins and the tubes are arranged in a triangular array. Cooling water flows inside the tubes. A displacer rod located inside each tube enhances the heat transfer by increasing the flow velocity. Helium flows on the outside of the tubes, countercurrent to the water flow.

### **4.5 Future Work**

In order to complete this model of the PCU, it will require the appropriate performance maps for the turbine and the compressors, inertia of the rotating parts, and more detail geometry of the heat transfer surfaces and flow channels in the heat exchangers. Once the stand-alone models are ready the next step is to integrate the components into one system and have all rotating parts on one shaft.

### **4.6 References**

- [4-1] Cheng, L., Ludewig, H. and Jo, J., "Passive Decay Heat Removal for a 2400 MW Pin Core by Natural Circulation," BNL report submitted to the DOE GEN-IV Program, January 2005.
- [4-2] Cheng, L. and Ludewig, H., "Analysis Of Depressurization Accident for a 2400 MW Gas Cooled Reactor – Effects of the Reactor Cavity Cooling System," BNL report submitted to the DOE GEN-IV Program, April 15 2005.
- [4-3] "Gas Turbine-Modular Helium Reactor (GT-MHR) Conceptual Design Description Report," General Atomics Report 910720 Revision 1, GA Project No. 7658, July 1996.
- [4-4] Kiryushin, A.I., et. al., "Project of the GT-MHR High-Temperature Helium Reactor with Gas Turbine," Nuclear Engineering and Design 173, p. 119-129, 1997.
- [4-5] Personal communication with D. Carosella of GA, Mathcad worksheet, PCUVOL.mcd, December 1, 2004.
- [4-6] Golovko, V.F., et. al., "Features of Adapting Gas Turbine Cycle and Heat Exchangers for HTGRs," Gas Turbine Power Conversion Systems for Modular HTGRs, IAEA-TECDOC-1238, p. 63-74, August 2001.
- [4-7] Kostin, V.I., et. al., "Power Conversion Unit with Direct Gas-Turbine Cycle for Electric Power Generation as a Part of GT-MHR Reactor Plant," Proceedings of the Conference

on High Temperature Reactors, #Paper D21, IAEA HTR-2004, Beijing, China, September 22-24, 2004.

- [4-8] “Review of the Gas Turbine-Modular Helium Reactor (GT-MHR) Plant,” Current Status and Future Development of Modular High Temperature Gas Cooled Reactor Technology, IAEA-TECDOC-1198, Chapter 4, February 2001.
- [4-9] Bikh, O.A., et. al., “Experimental Investigation of High-Temperature High-Performance Recuperator,” Proceedings of the Conference on High Temperature Reactors, #Paper H10, IAEA HTR-2004, Beijing, China, September 22-24, 2004.
- [4-10] Bikh, O.A., et. al., “Design and Experiment Investigations of Compact Recuperators for Reactor Plants with Gas-Turbine Cycle,” Proceedings of the Conference on High Temperature Reactors, #Paper H11, IAEA HTR-2004, Beijing, China, September 22-24, 2004.
- [4-11] Bikh, O.A., et. al., “Experimental Investigation for the Optimization of Powerful Turbine Plants Gas Coolers Heat Exchange Surface Ribbing,” Proceedings of the Conference on High Temperature Reactors, #Paper H09, IAEA HTR-2004, Beijing, China, September 22-24, 2004.



## 5. Conclusions and Recommendations

The current reference design of the GFR operates at a relatively high power density, but has very little thermal inertia to aid in decay heat removal during accident conditions. The low thermal inertia, coupled with a working fluid that has poor heat transfer characteristics, creates a major challenge for the GFR with respect to passive decay heat removal during accident conditions; specifically for loss-of-coolant and loss-of-flow accidents. Conductive and radiative heat transfer alone cannot effectively remove the decay heat, where natural convective cooling is also needed if passive systems are to remain as a viable option.

Based on the work performed to date on safety system design for decay heat removal, the following conclusions can be made:

1. A fully passively safe GFR design is possible with low power density, but the economics can be prohibitive.
2. To reduce the economic burden of a fully passively safe system, a backpressure is needed to enhance natural convective cooling during off-normal events. The higher the backpressure, the more effective the cooling based on the main driving force for natural convection: mass flow. Thus increased mass (or higher pressure) enhances natural convection. However, the containment must withstand these pressures for extended periods of time, which would require a higher cost for the containment. Conversely, a guard (or secondary) vessel could be designed to withstand the needed backpressure at a lower cost. (This report focuses on this safety system design variant.)
3. Heavy gas injection enhances natural convection, and reduces the backpressure needed to remove the decay heat due to the increased mass of the working fluid.
4. While not passive, use of active systems require very little power ( $\sim 100\text{kW} \times 3$ ), where their reliability may be better than their passive counterparts.
5. Active/passive combined systems require a minimal backpressure, and only  $\sim 16\text{kW} (x 3)$  for the active side. As stated earlier in this report, this scenario would require that a blower is run for the first 24 hours of an accident, at which point it can be shut down to allow solely natural convective cooling to occur for the remainder of the accident period.

The GFR research effort has been focused on items 2 and 5 to maintain the ideals of using passive safety as much as is reasonably achievable given the other Generation IV goals. However, as shown within this report, other issues will need further study (e.g., cooling the guard containment reduces the pressure of the working fluid, which decreases the effective cooling of the core). Future work will focus on the trade-offs within items 2 and 5, and work will begin on more detailed analyses of using item 3 and its trade-offs. In addition, related U-NERI work will take a preliminary look at the reliability aspects of item 4, which will also affect item 5.